

Development of particle multiplicity distributions using a general form of the grand canonical partition function and applications to L3 and H1 Data

S.J. Lee

Department of Physics and Institute of Natural Sciences, Kyung Hee University, Suwon, KyungGiDo, Korea

A.Z. Mekjian

Department of Physics, Rutgers University, Piscataway, New Jersey

Various phenomenological models of particle multiplicity distributions are discussed using a general form of a unified model which is based on the grand canonical partition function and Feynman's path integral approach to statistical processes. These models can be written as special cases of a more general distribution which has three control parameters which are a , x , z . The relation to these parameters to various physical quantities are discussed. A connection of the parameter a with Fisher's critical exponent τ is developed. Using this grand canonical approach, moments, cumulants and combinants are discussed and a physical interpretation of the combinants are given and their behavior connected to the critical exponent τ . Various physical phenomena such as hierarchical structure, void scaling relations, KNO scaling features, clan variables, and branching laws are shown in terms of this general approach. Several of these features which were previously developed in terms of the negative binomial distribution are found to be more general. Both hierarchical structure and void scaling relations depend on the Fisher exponent τ . Applications of our approach to the charged particle multiplicity distribution in jets of L3 and H1 data are given. It is shown that just looking at the mean and fluctuation of data is not enough to distinguish these distributions or the underlying mechanism. The mean, fluctuation and third cumulant of distribution determine three parameters x , z , a . We find that a generalized random work model fits the data better than the widely used negative binomial model.

I. INTRODUCTION

Pion multiplicity distribution and their associated fluctuation and correlations have been of interest for several reasons. Several models predict large fluctuations such as the disoriented chiral condensate [1,2] and in density fluctuations from droplets arising in a first order phase transition [3]. A well known procedure for studying correlations uses the Bose-Einstein symmetries associated with pions in a Hanbury Brown-Twiss analysis [4]. Such an analysis gives information about the space time history of the collision through measurements of source parameters. If the density of pions becomes large, Bose-Einstein correlation may also lead to a strongly emitting system which has been called a pion laser [5]. The pion laser model has been recently solved analytically by T. Csörgö and J. Zimanyi [6]. The importance of Bose-Einstein correlations has also been illustrated in the observation of a condensation of atoms in a harmonic oscillator or laser trap [7]. Previous interest in pionic distributions have centered around the possibility of intermittency behavior [8] and fractal structure based on parallels with turbulent flow in fluids. A distribution widely used to discuss such features has been the negative binomial (NB) distribution [9] with its associated clan structure [10,11] and KNO scaling feature [12]. KNO scaling properties have been interpreted in terms of a phase transition associated with a Feynman-Wilson gas [13]. Various other issues associated with pions include evidence for thermalization [14], critical point fluctuations [15,16], fluctuations from a first order phase transition [17], charge particle ratios and question of chemical equilibrium [18], the behavior of fluctuations in net charge in a QG plasma for transition [19,20].

For lower energy heavy ion collisions, multifragmentation of nuclei takes place. The fragment distribution can also be described statistically by considering all the possible partition of A nucleons into smaller clusters [21,22]. This study gives a tool for the description of nuclear multifragmentation distributions [23], nuclear liquid-gas phase transition [24], critical exponent, intermittency, and chaotic behavior [25,26] of nuclear multifragmentation. The same model can describe pionic distribution. This possibility arises in our approach which is based on Feynman path integral methods where symmetrization of A bosons or anti-symmetrization of A fermions leads to a cycle class decomposition of the permutations associated with these symmetries. The correspondance comes from the identification of clusters of size k and the cycles of length k in a permutation as discussed below. In nuclear multifragmentation the number of nucleons, A , is fixed and thus a canonical partition function approach is appropriate. By contrast, the number of

pions, A , in particle production is not fixed and thus we need to use a grand canonical partition. Using this parallel, we also note that some results from cluster yields can be carried over into particle multiplicity distributions and associated properties. Namely, we show the importance of the Fisher critical exponent τ and relate it to one of the parameters called a in our approach which has three main parameters a, x, z . Moreover, taking special values of a , or equivalently τ , reduces our unified model to various specific cases that are frequently used in particle production phenomenology. Quantities that appear in this development can also be related combinants as will be discussed. In so doing we can give a physical significance to the combinants and show how the Fisher exponent appears in them and how the resulting hierarchical structure and void scaling relations also depend on its value.

In next section a summary of a generalized statistical model based on a grand canonical partition function will be given. This generalized model can be used to study multiplicity distributions associated with particle production such as at RHIC. Various models of particle multiplicity distribution using the grand canonical partition function will then be developed. In Section II-B, we will summarize the multiplicity distribution and its various moments of all order for a general grand canonical ensemble which we will then use for particle production. The physical meaning of the parameters used in this model is given here. The differences and relations between the canonical nuclear multifragmentation and the grand canonical multiparticle production are summarized in Sect. II-C. In Sect. II-D and E, moments (especially the mean and the fluctuation) in the general grand canonical model are related to variables used in other existing standard models in describing multiparticle production. The connection of the general grand canonical model developed here to existing standard models are summarized in Sect. II-F. Moreover, we derive a generalized model (HGa) of the grand canonical partition which can further be reduced to a geometric, negative binomial, and Lorentz/Catalan model. Various moments and multiplicity distribution for a generalized HGa model are summarized in Sect. II-G and another generalized model (GRW1D) in Sect. II-H. In Sect. III, we compare various statistical properties between different models within the generalized HGa model and with data for charged particle distribution in jets of L3 and H1. Fluctuation and multiplicity distribution in HGa are compared with other standard models of multiparticle production.

II. GENERALIZED PROBABILITY DISTRIBUTIONS

Consider a system composed of N different types of species or objects which could be the fragments in a fragmentation or in a cycle class description. Any event of such a system can be associated with a vector $\vec{n} = \{n_k\} = (n_1, n_2, \dots, n_k, \dots, n_N)$ or $1^{n_1} 2^{n_2} 3^{n_3} \dots k^{n_k} \dots N^{n_N}$ where the non-negative integer n_k is the number of individuals of species k . For example n_k can be the number of clusters of size k or the number of cycles of length k in a given permutation of n particles. The later is important for Bose-Einstein and Fermi-Dirac statistics and particle multiplicity distributions. A general block picture of \vec{n} is shown in Fig.1a. Fig.1b shows how the various partition can be developed as an evolution from successively smaller systems. The number of species N can be infinity in general.

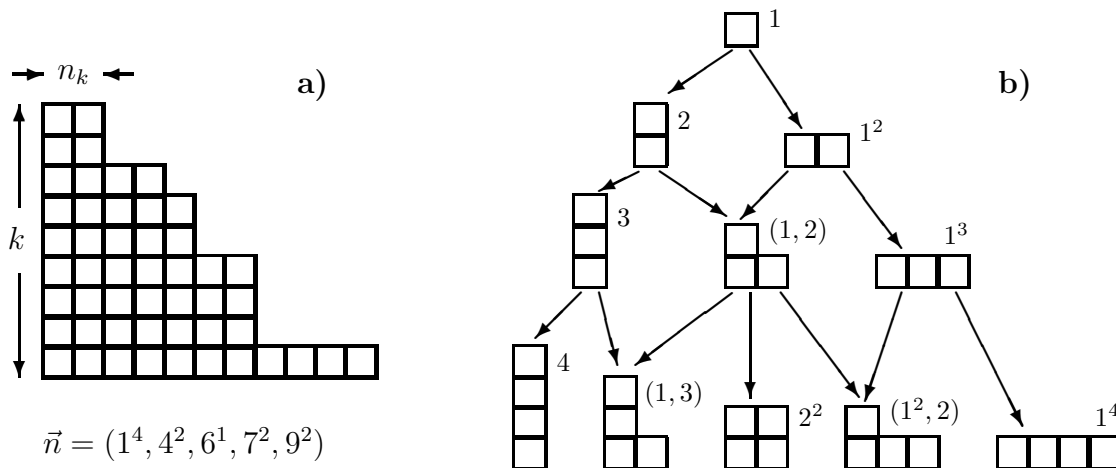


FIG. 1. Building partitions with blocks.

Various probability distributions related with this system can be developed by assigning an appropriate weight x_k to each type k . A weight $W(\vec{x}, \vec{n})$ is then given to each event \vec{n} and the type of weight that will be considered has the structure:

$$W(\vec{x}, \vec{n}) = \prod_{k=1}^N \left[\frac{x_k^{n_k}}{n_k!} \right] \quad (1)$$

The $n_k!$ are Gibbs factorials. Such a weight structure appears in Feynman's path integral approach and Bose-Einstein problems [27]. The x_k will be given below and contains various physical quantities. In Sect.IIB we will show that the x_k 's are also the combinants which in turn can be related to the factorial cumulants. Summing the weight $W(\vec{x}, \vec{n})$ over all the possible events of \vec{n} , the grand canonical partition function $Z(\vec{x})$ of the system is given as

$$Z(\vec{x}) = \sum_{\vec{n}} W(\vec{x}, \vec{n}) = \sum_{\vec{n}} \prod_{k=1}^N \left[\frac{x_k^{n_k}}{n_k!} \right] = \exp \left[\sum_{k=1}^N x_k \right] \quad (2)$$

The last equation holds due to the form of Eq.(1) of the weight $W(\vec{x}, \vec{n})$, i.e., the factor $x_k^{n_k}/n_k!$ is the n_k -th order expansion term of e^{x_k} .

Introducing other quantities α_k to each individual entity or group of type k , $\vec{\alpha} = \{\alpha_k\} = (\alpha_1, \alpha_2, \dots, \alpha_k, \dots, \alpha_N)$, we can define a canonical partition function $Z_A(\vec{x})$ with a fixed A as

$$A = \sum_{k=1}^N \alpha_k n_k = \vec{\alpha} \cdot \vec{n} \quad (3)$$

$$Z_A(\vec{x}) = \sum_{\vec{n}_A} W(\vec{x}, \vec{n}) = \sum_{\vec{n}_A} \prod_{k=1}^N \left[\frac{x_k^{n_k}}{n_k!} \right] \quad (4)$$

with $Z(\vec{x}) = \sum_A Z_A(\vec{x})$. Here $\sum_{\vec{n}_A}$ is the summation over all events with a fixed value of A , i.e., over a canonical ensemble of a fixed A , and the \sum_A is a summation over all the possible values of A ; it becomes $\sum_{A=0}^{\infty}$ for the case of $\alpha_k = k$ with positive integer k . The multiplicity of a partitions is

$$M = \sum_{k=1}^N n_k \quad (5)$$

The case $\alpha_k = k$ is encountered in fragmentation problems and permutation problems. Various type of α_k can be used depending on the physics related with the quantity A as discussed in Ref. [22]. The physics of the canonical ensemble depends on the choice of the quantity α_k [21,22]. If we take $x_k \propto z^{\alpha_k}$, then the canonical partition function $Z_A(\vec{x})$ is the z^A dependent term of the grand canonical partition function $Z(\vec{x})$. If we take $x_k \propto x$, then x counts the number of clusters M explicitly and the x^M dependent term of the grand canonical partition function $Z(\vec{x})$ is the partition function for events with multiplicity M . There always is at least one event having $A = 0$, i.e., the event where all n_k 's are zero, $\vec{n} = \vec{0}$. Thus $Z_0(\vec{x}) = 1$ if all α_k are non zero positive since then there are no other possible events having $A = 0$. Due to the form of the weight $W(\vec{x}, \vec{n})$ given by Eq.(1) the canonical partition function $Z_A(\vec{x})$ satisfies a recurrence relation [25,27]

$$Z_A(\vec{x}) = \frac{1}{A} \sum_k \alpha_k x_k Z_{A-\alpha_k}(\vec{x}) \quad (6)$$

This relation is nothing but the constraint Eq.(3) in terms of the mean $\langle n_k \rangle_A$ using Eq.(8). For non-zero positive α_k , there is no case having $A < 0$, i.e., $Z_A = 0$ for $A < 0$ and thus the Z_A can be obtained by the recurrence relation of Eq.(6) starting from $Z_0(\vec{x}) = 1$.

A. Probability distribution

In a canonical ensemble of fixed A , we can define a probability distribution of a specific partition \vec{n} as

$$P_A(\vec{x}, \vec{n}) = \frac{W(\vec{x}, \vec{n})}{Z_A(\vec{x})} \quad (7)$$

With this probability, various mean values, fluctuations and correlations of the number of species n_k can be evaluated as a ratio of canonical partition functions for two different values of A such as [21,22]

$$\left\langle \frac{n_k!}{(n_k - m)!} \frac{n_j!}{(n_j - l)!} \right\rangle_A = \sum_{\vec{n}_A} \frac{n_k!}{(n_k - m)!} \frac{n_j!}{(n_j - l)!} P_A(\vec{x}, \vec{n}) = x_k^m x_j^l \frac{Z_{A-m\alpha_k-l\alpha_j}(\vec{x})}{Z_A(\vec{x})} \quad (8)$$

Thus we have $\langle n_k \rangle_A = x_k \frac{Z_{A-\alpha_k}(\vec{x})}{Z_A(\vec{x})}$. The recurrence relation of Eq.(6) then follows simply using the fact that $A = \sum_{k=1}^N \alpha_k \langle n_k \rangle$. This distribution has been used in describing various fragment distributions in nuclear multi-fragmentation [21–23].

Now knowing the partition functions $Z(\vec{x})$ and $Z_A(\vec{x})$, we can associate a probability $P_A(\vec{x})$ of the system to have a fixed value of A in a grand canonical ensemble as

$$P_A(\vec{x}) = \frac{Z_A(\vec{x})}{Z(\vec{x})} = \frac{1}{Z(\vec{x}) \Gamma(A+1)} \left[\left(\frac{d}{dz} \right)^A Z(\vec{x}, z) \right]_{z=0} \quad (9)$$

$$Z(\vec{x}, z) = \sum_A Z_A(\vec{x}) z^A = \exp \left[\sum_k x_k z^{\alpha_k} \right] \quad (10)$$

The last step follows from the fact that the z^A power term of $Z(\vec{x}, z)$ is $Z_A(\vec{x})$ if we put $x_k = z^{\alpha_k}$. For particle production $P_A(\vec{x})$ is the probability of having A particles. Thus the generating function $Z(\vec{x}, z)$ of P_A can also be looked at as a grand canonical partition function with the weight x_k replaced to be $x_k z^{\alpha_k}$, where the variable z counts A explicitly and $Z(\vec{x}, 1) = Z(\vec{x})$. If we consider $P_A(\vec{x}, z) = P_A(\vec{x}) z^A$ then z has two roles; one as a weight which is assigned the same to each constituent and another as a generating parameter of the probability $P_A(\vec{x})$. For the case that $Z_0(\vec{x}) = 1$, the void probability P_0 [28] is the inverse of the grand canonical partition function, i.e.,

$$P_0(\vec{x}) = \frac{Z_0(\vec{x})}{Z(\vec{x})} = Z^{-1}(\vec{x}) \quad (11)$$

Inversely the canonical partition function $Z_A(\vec{x})$ is the probability P_A normalized or rescaled by the void probability P_0 , i.e.,

$$Z_A(\vec{x}) = \frac{1}{\Gamma(A+1)} \left[\left(\frac{d}{dz} \right)^A Z(\vec{x}, z) \right]_{z=0} = \frac{P_A(\vec{x})}{P_0(\vec{x})} \quad (12)$$

Another type of generating function of P_A that is frequently used may be defined as

$$\begin{aligned} G(\vec{x}, u) &= \sum_A P_A(\vec{x}) (1-u)^A = \frac{1}{Z(\vec{x})} \sum_A Z_A(\vec{x}) (1-u)^A \\ &= \frac{Z(\vec{x}, z=1-u)}{Z(\vec{x})} = \exp \left[\sum_k x_k [(1-u)^{\alpha_k} - 1] \right] \end{aligned} \quad (13)$$

$$P_A(\vec{x}) = \frac{1}{\Gamma(A+1)} \left[\left(-\frac{d}{du} \right)^A G(\vec{x}, u) \right]_{u=1} \quad (14)$$

We see that $G(\vec{x}, 0) = 1$, $G(\vec{x}, 1) = P_0(\vec{x}) = Z_0(\vec{x})/Z(\vec{x})$ and $G(\vec{x}, 1-z) = Z(\vec{x}, z)/Z(\vec{x})$. Once the probability $P_A(\vec{x})$ is determined, various statistical quantities can be evaluated. Also the grand canonical partition function $Z(\vec{x}, z)$ is given once we know the thermodynamic grand potential

$$\Omega(\vec{x}, z) = -\ln Z(\vec{x}, z) = -\sum_k x_k z^{\alpha_k}. \quad (15)$$

This result can be used to study the statistical properties of a system. Moreover various moments and cumulants, mean values and fluctuations may be obtained using the generating function [21,22].

B. Moments and cumulants; combinants and hierachical structure in grand canonical ensemble

This subsection gives general expression for various quantities that will be used later when we discuss specific models. Since the probability of a specific event \vec{n} in a grand canonical ensemble is given by

$$P(\vec{x}, \vec{n}) = \frac{W(\vec{x}, \vec{n})}{Z(\vec{x})} = \sum_A P_A(\vec{x}) P_A(\vec{x}, \vec{n}) \quad (16)$$

the mean of a quantity F in a grand canonical ensemble is related to the mean of F in a canonical ensemble as

$$\langle F \rangle = \sum_{\vec{n}} F P(\vec{x}, \vec{n}) = \sum_A P_A(\vec{x}) \sum_{\vec{n}_A} F P_A(\vec{x}, \vec{n}) = \sum_A P_A(\vec{x}) \langle F \rangle_A \quad (17)$$

We can easily show that

$$\langle n_k \rangle = \sum_{\vec{n}} n_k P(\vec{x}, \vec{n}) = \sum_A P_A(\vec{x}) \langle n_k \rangle_A = x_k \quad (18)$$

$$\langle M \rangle = \sum_{\vec{n}} \left(\sum_k n_k \right) P(\vec{x}, \vec{n}) = \sum_k x_k = -\Omega(\vec{x}, z=1) \quad (19)$$

This result shows that the weight factor x_k in this model is the mean number $\langle n_k \rangle$ in a grand canonical ensemble and that the mean multiplicity $\langle M \rangle$ is related to the thermodynamic potential. The m -th power moment of A and its factorial moments are given simply by

$$\langle A^m \rangle(\vec{x}) \equiv \sum_{\vec{n}} \left(\sum_{k=1}^N \alpha_k n_k \right)^m P(\vec{x}, \vec{n}) = \frac{1}{Z(\vec{x})} \left[\left(z \frac{d}{dz} \right)^m Z(\vec{x}, z) \right]_{z=1} \quad (20)$$

$$\left\langle \frac{\Gamma(A+1)}{\Gamma(A-m+1)} \right\rangle(\vec{x}) \equiv \sum_{\vec{n}} \frac{\Gamma(A+1)}{\Gamma(A-m+1)} P(\vec{x}, \vec{n}) = \frac{1}{Z(\vec{x})} \left[\left(\frac{d}{dz} \right)^m Z(\vec{x}, z) \right]_{z=1} \quad (21)$$

Similarly the m -th cumulants, which is the power moments of α_k , and the factorial cumulants are

$$\langle \alpha^m \rangle(\vec{x}) \equiv \left\langle \sum_{k=1}^N \alpha_k^m n_k \right\rangle = \left[\left(z \frac{d}{dz} \right)^m \ln Z(\vec{x}, z) \right]_{z=1} = \sum_{k=1}^{\infty} \alpha_k^m x_k \quad (22)$$

$$\begin{aligned} f_m(\vec{x}) &\equiv \left\langle \sum_{k=1}^N \frac{\Gamma(\alpha_k+1)}{\Gamma(\alpha_k-m+1)} n_k \right\rangle = \left[\left(\frac{d}{dz} \right)^m \ln Z(\vec{x}, z) \right]_{z=1} \\ &= \left[\left(-\frac{d}{du} \right)^m \ln G(\vec{x}, u) \right]_{u=0} = \sum_{k=1}^N \frac{\Gamma(\alpha_k+1)}{\Gamma(\alpha_k-m+1)} x_k \end{aligned} \quad (23)$$

Due to Eqs.(10) and (15) we can see easily that, for the power moments of α_k ,

$$\langle \alpha^0 \rangle = \sum_{k=1}^N x_k = f_0 = \langle M \rangle \quad (24)$$

$$\langle \alpha^1 \rangle = \sum_{k=1}^N \alpha_k x_k = f_1 = \langle A \rangle \quad (25)$$

$$\langle \alpha^2 \rangle = \sum_{k=1}^N \alpha_k^2 x_k = f_2 + f_1 = \langle (A - \langle A \rangle)^2 \rangle = \langle A^2 \rangle - \langle A \rangle^2 = \sigma^2 \quad (26)$$

$$\langle \alpha^3 \rangle = \sum_{k=1}^N \alpha_k^3 x_k = f_3 + 3f_2 + f_1 = \langle (A - \langle A \rangle)^3 \rangle \quad (27)$$

The power moments of α_k are directly related to the power moments of A measured from the mean $\langle A \rangle$, i.e., the cumulants $\langle \alpha^m \rangle$ are same with the central moments of A . This simple relation does not hold for $m \geq 4$ but we can evaluate them starting from $\langle \alpha^3 \rangle$ using the recurrence relation

$$\langle \alpha^{m+1} \rangle(\vec{x}, z) = \left(z \frac{d}{dz} \right)^{m+1} \ln Z(\vec{x}, z) = \left(z \frac{d}{dz} \right) \langle \alpha^m \rangle(\vec{x}, z) \quad (28)$$

Similarly the m -th factorial cumulants f_m , which is the factorial moments of α_k , can be found using recurrence relation

$$\frac{f_{m+1}(\vec{x}, z)}{f_m(\vec{x}, z)} = z \left(\frac{d}{dz} \right) \ln f_m(\vec{x}, z) - m \quad \text{or} \quad \frac{f_m(\vec{x}, z)}{z^m} = \frac{d}{dz} \left(\frac{f_{m-1}(\vec{x}, z)}{z^{m-1}} \right) = \left(\frac{d}{dz} \right)^m f_0(\vec{x}, z) \quad (29)$$

starting from

$$f_0(\vec{x}, z) = \langle M \rangle(\vec{x}, z) = \ln Z(\vec{x}, z) = -\Omega(\vec{x}, z) = \sum_{k=1}^N x_k z^{\alpha_k} \quad (30)$$

$$f_1(\vec{x}, z) = \langle A \rangle(\vec{x}, z) = \sum_{k=1}^N \alpha_k x_k z^{\alpha_k} \quad (31)$$

The reduced factorial cumulants κ_m defined in Ref. [28] corresponds to the factorial cumulants f_m normalized with mean number $\langle A \rangle = \bar{A}$ as

$$\kappa_m(\vec{x}, z) = \frac{f_m(\vec{x}, z)}{\bar{A}^m} \quad (32)$$

Thus with $\kappa_1 \equiv 1$ and $\kappa_0 = f_0 = \langle M \rangle$. The cummulants are directly related with the generating functions as

$$G(\vec{x}, u) = \exp \left[\sum_{m=1}^{\infty} \frac{(-u)^m}{m!} f_m(\vec{x}) \right] = \exp \left[\sum_{m=1}^{\infty} \frac{(\ln[1-u])^m}{m!} \langle \alpha^m \rangle(\vec{x}) \right] \quad (33)$$

$$Z(\vec{x}, z) = \exp \left[\sum_{m=0}^{\infty} \frac{(z-1)^m}{m!} f_m(\vec{x}) \right] = \exp \left[\sum_{m=0}^{\infty} \frac{(\ln z)^m}{m!} \langle \alpha^m \rangle(\vec{x}) \right] \quad (34)$$

The generating function $Z(\vec{x}, z)$ differs from the generating function $G(\vec{x}, u = 1 - z)$ only by an extra term of $m = 0$ in their exponent.

The relation between the x_k 's and the Z shows that the x_k 's are also the combinants of Ref. [29]. In the approach presented here, the combinants are given an underlying significance through the partition weight $W(\vec{x}, \vec{n})$ of Eq.(1). In turn the combinants x_k can be related to the factorial cumulants f_m defined by

$$\ln Z(\vec{x}, z) = \sum_k x_k z^{\alpha_k} = \sum_{m=0}^{\infty} \frac{(z-1)^m}{m!} f_m(\vec{x}) \quad (35)$$

The factorial cumulants f_m are the m -th order factorial moments of α_k of Eq.(23). Thus

$$f_m = m! \sum_{k=m}^{\infty} \binom{k}{m} x_k \quad (36)$$

for $\alpha_k = k$ which is the Eq.(23) with $N \rightarrow \infty$. The normalized factorial cumulant, i.e., the reduced cumulant, is

$$\kappa_m = f_m / \bar{A}^m = (m-1)! \kappa_2^{m-1} \quad (37)$$

for a negative binomial (NB) distribution, This result of Eq.(37) shows that κ_m for NB has an hierarchical structure of a distribution at the reduced cumulant level which was realized for the NB distribution in Ref. [28]. This result will be generalized later.

Also using the above power moments and factorial moments we can study voids and void scaling relation, hierarchical structure, combinant and cummulant properties which will be discussed below.

C. Multi-fragmentation versus multiparticle production and the Fisher exponent for particle production

Since our approach was first used to discuss multifragmentation and then later extended to include multiparticle production, we briefly mention some of difference between multifragmentation and multiparticle production. We also show how the Fisher exponent τ , which initially appeared in cluster yields around a critical point, may manifest itself in particle production yields.

In nuclear multifragmentation, $\alpha_k = k$ is the number of nucleons in a fragment and n_k is the number of fragments of size k . The total number of fragments is $M = \sum_k n_k$ and the total number of nucleons is $A = \sum_k kn_k$. In nuclear multifragmentation, the total number of nucleons A is usually fixed and we study the distribution in size k of the mean multiplicity $\langle n_k \rangle_A = x_k Z_{A-k}(\vec{x})/Z_A(\vec{x})$ of fragments of size k in a canonical ensemble. In multiparticle production the A is the total number (multiplicity) of produced particles and is not fixed and we study the multiplicity distribution of produced particles $P_A = Z_A(\vec{x})/Z(\vec{x})$ as a function of A in a grand canonical ensemble. The mean multiplicity $\langle M \rangle_A$ and $\langle n_k \rangle_A$ in a canonical ensemble are related with grand canonical ensemble as

$$\begin{aligned}\langle n_k \rangle &= \sum_{A=0}^{\infty} \langle n_k \rangle_A P_A = x_k \\ \langle M \rangle &= \sum_{A=0}^{\infty} \langle M \rangle_A P_A = \sum_k x_k \\ \langle A \rangle &= \sum_{A=0}^{\infty} \sum_k k \langle n_k \rangle_A P_A = \sum_{A=0}^{\infty} A P_A = \sum_k k x_k\end{aligned}$$

The weight x_k can be determined experimentally from the mean multiplicity $\langle n_k \rangle$ of cluster size k in a grand canonical ensemble.

In our initial fragmentation studies [21–23] we have used $x_k = xz^k/k$. This choice gives $Z_A(x, z) = (z^A/A!) \Gamma(x + A)/\Gamma(x)$ and thus $Z_{A-k}/Z_A \rightarrow z^{-k}$ as $A \rightarrow \infty$ where the $z = e^{\beta\mu}$ with μ the chemical potential. From Eq.(8), $\langle n_k \rangle_A = x_k Z_{A-k}/Z_A$, thus $\langle n_k \rangle_A \rightarrow x/k$ as $A \rightarrow \infty$ in the case of nuclear fragmentation in the canonical ensemble of fixed A for $x_k = xz^k/k$ and the yields fall as a power law $1/k$ at a critical point ($x = 1$) for this choice of x_k . The yield in the grand canonical ensemble is $\langle n_k \rangle = x_k = xz^k/k$ and this becomes the same as $\langle n_k \rangle_A \rightarrow x/k$ in $A \rightarrow \infty$ limit for $z = 1$ with $\mu = 0$. In general, cluster yields fall for large k as a power law $1/k^\tau$ at a critical point where τ is the Fisher critical exponent. The above choice of x_k can be generalized to $x_k = xz^k/k^\tau$ so that the cluster yields fall as $1/k^\tau$. The τ determines the grand canonical partition function $Z(\vec{x}) = \exp[\sum_k x_k] = \exp[x \sum_k z^k/k^\tau]$. Forms for x_k whose asymptotic behavior is xz^k/k^τ can also be used. In section II.F we will give various choice for x_k for particle production. For example, the above choice of x_k with $\tau = 1$ gives the frequently used negative binomial distribution with x the negative binomial parameter which determines the degree of departure from Poisson statistics. Other distributions can be generated and their associated τ dependence will also be given. Then we will show how the τ dependence of the combinants shows up in hierarchical structure and void scaling relations in sect II.G and in other places. The physical meaning of x and z will also be discussed for these other cases. Since an exact description of particle multiplicity yields is not known, we consider τ as a free exponent to be determined by comparing various resulting distributions with experiment. This procedure is what is done in cluster yields. In multi-fragmentation distribution, the mean number of clusters $\langle M \rangle$ is determined by x and z is directly related with the number of constituent particles A . The large k behavior of the mean number of cluster $\langle n_k \rangle$ gives the Fisher power τ . In multiparticle distribution, x and z determine the mean particle number $\langle A \rangle$ or the peak position of the particle number distribution P_A and the fluctuation $\sigma^2 = \langle A^2 \rangle - \langle A \rangle^2$ or the width of the particle distribution. The Fisher power τ determines the large k behavior of the weight x_k and offers a new parameter in particle production. $\langle n_k \rangle = x_k$ in grand canonical ensemble.

Bose-Einstein condensation of atoms in a box of sides L of dimensions d have $x = L^d/\lambda_T^d$ with $\lambda_T = h/(2\pi mk_B T)^{1/2}$ and have $\tau = 1 + d/2$. Feynman used random walk arguments, the closing of a cycle parallels a closed random walk, to discuss his choice of x_k in his discussion of a superfluid phase transition in liquid helium. Thermal emission of pions based on statistical mechanics and equilibrium ideas have been popular descriptions of pions coming from relativistic heavy ion collisions. For thermal models [30], the $x_k = (VT^3/2\pi^2)(m/T)^2 K_2(km/T)/k$ for a cycle length k or a cluster of size k with K_2 a Mac Donald function. For low temperatures, $x_k = (V/\lambda_T^3)(e^{-m/T})^k/k^{5/2}$ and the Boltzmann factor in mass, $e^{-km/T}$, suppresses large fluctuations. In the high temperature limit and/or zero pion mass limit $x_k = (V/\pi^2)T^3/k^4$. Thus the high temperature limit has $\tau = 4$ and the low temperature limit has $\tau = 5/2$. The x_k can be used to generate the pion probability distribution P_n . The thermal models can be combined with hydrodynamic descriptions and an application was given [30] to 158A GeV Pb+Pb data measured by the CERN/NA44

and CERN/NA49 collaborations. The results of Ref. [30] showed a Gaussian distribution with a width about 20 % larger than the Poisson result.

D. Clan parameters and void parameters and void scaling relations

Van Hove and Giovannini have introduced clan variables N_c and n_c to describe a general class of probability distributions, with most discussions of these variables centering around the negative binomial distribution [11]. These variables are defined as

$$N_c = \langle M \rangle = \ln Z = f_0, \quad n_c = \langle A \rangle / N_c = f_1 / f_0 \quad (38)$$

where the mean number of clans is N_c and the n_c is the mean number of members per clan. The Z is the grand canonical generating function and thus $N_c = \sum_k x_k$ where x_k is the cycle class weight distribution \vec{x} . The $\langle A \rangle = \sum_k k \langle n_k \rangle$ is the mean number of total members (particles). The n_k here is the number of clans of size k having k members.

The clan variable N_c is also related to the void probability $P_0 = Z_0/Z = 1/Z = e^{-N_c}$; thus $N_c = -\ln P_0 = f_0$. An important function in void analysis is $\chi = -\ln P_0 / \langle A \rangle = N_c / \langle A \rangle = 1/n_c$. Thus the void parameters, void probability P_0 and void function $\nu = \chi$ [28], are equivalent to the generalized clan parameters N_c and n_c with the equivalence given by:

$$f_0(\vec{x}) = \ln Z(\vec{x}) = -\ln P_0(\vec{x}) = N_c \quad (39)$$

$$\chi(\vec{x}) \equiv \frac{f_0(\vec{x})}{\langle A \rangle} = \nu = n_c^{-1} \quad (40)$$

The $-\chi$ is the normalized grand potential $\Omega = -f_0$ for the mean $\langle A \rangle$.

Void analysis looks for scaling properties associated with χ ; specifically, χ is a function of the combination $\langle A \rangle \xi$ where ξ is the coefficient of $\langle A \rangle^2$ in the fluctuation $\sigma^2 = \langle A \rangle + \xi \langle A \rangle^2$. Since $f_2 = \langle \alpha^2 \rangle - \langle \alpha \rangle = \langle (A - \langle A \rangle)^2 \rangle - \langle A \rangle$, the variance of A in a grand canonical ensemble becomes

$$\begin{aligned} \sigma^2 &\equiv \langle A^2 \rangle - \langle A \rangle^2 = \langle \alpha^2 \rangle = \sum_k \alpha_k^2 x_k \\ &= \langle A \rangle + f_2 = \langle A \rangle + \xi \langle A \rangle^2 = \langle A \rangle [1 + \xi(\vec{x}) \langle A \rangle] \end{aligned} \quad (41)$$

with $\xi = \kappa_2$, i.e., the normalized factorial cumulant. Since the variance for a Poissonian distribution is the same as the mean, $\sigma^2 = \langle A \rangle$, the $\xi = 0$; thus, the parameter $\xi \langle A \rangle$ represents a degree of departure from Poissonian fluctuation normalized by mean $\langle A \rangle$ of the distribution. A well known non-Poissonian example is a NB distribution which has $\xi = \frac{1}{x}$ and this becomes Plank distribution with $x = 1$. Thus the variable x in x_k determines the strength of the non-Poissonian fluctuation term for the negative binomial distribution. In general, x and z determine the mean particle number or the peak position of the particle multiplicity distribution and the fluctuation or the width of the particle distribution. Using the recurrence relation Eq.(29) for f_m , we can show that

$$\xi(\vec{x}, z) \langle A \rangle(\vec{x}) = \chi^{-1}(\vec{x}, z) - z \left(\frac{d}{dz} \right) \ln \chi(\vec{x}, z) - 1 = \frac{1 - z \left(\frac{d}{dz} \right) \chi(\vec{x}, z)}{\chi(\vec{x}, z)} - 1 \quad (42)$$

$$\kappa_3(\vec{x}, z) = \frac{f_3(\vec{x}, z)}{\langle A \rangle^3} = \frac{\xi(\vec{x}, z)}{\langle A \rangle} \left(z \frac{d}{dz} \right) \ln [\xi(\vec{x}, z) \langle A \rangle^2] - 2 \frac{\xi(\vec{x}, z)}{\langle A \rangle} \quad (43)$$

A NB distribution has $\chi = \ln(1 + \xi \langle A \rangle) / (\xi \langle A \rangle)$ while the Lorentz/Catalan (LC) distribution discussed in Ref. [31] and below has $\chi = (\sqrt{2\xi \langle A \rangle + 1} - 1) / (\xi \langle A \rangle)$. We will study in Sect. III A, χ vs $\xi \langle A \rangle$, i.e., the void or clan variable vs the fluctuation for various choices of x_k summarized in Table I.

E. Ancestral or evolutionary variables

The LC model, which has $x_k = \frac{1}{k} 2^{-2(k-1)} \binom{2(k-1)}{k-1} x z^k$, was shown to be a useful model for discussing an underlying splitting dynamics when ancestral or evolutionary variables p and β were introduced into x and z as discussed in Ref. [31]. Specifically $x = \beta/4p$ and $z = 4p(1-p)$ giving $x_k = \beta C_k p^{(k-1)} (1-p)^k$ where $C_k = \frac{1}{k} \binom{2(k-1)}{k-1}$.

Percolation or splitting dynamics with a branching probability p and survival probability $(1-p)$ has a hierarchical topology as shown in Fig.2. Weighting each diagram by $x_k = \beta C_k p^{k-1} (1-p)^k$, the evolutionary or ancestral variables are related to the clan variables $N_c = \langle M \rangle$ and $n_c = \langle A \rangle / N_c$. C_k is the number of diagrams of size k shown in Fig.2. For this case the evolutionary dynamics is just that of the LC model. Then with β set equal to 1, $x_1 = (1-p)$, $x_2 = p(1-p)^2$, $x_3 = 2p^2(1-p)^3$, $x_4 = 5p^3(1-p)^4$, etc. The interpretation of this set of x_k 's reads as follows: x_1 has 1 surviving line without a branch ($p^0(1-p)^1$) and one diagram ($C_1 = 1$), x_2 has 1 branch (p^1) leading to 2 surviving lines ($(1-p)^2$) and one diagram ($C_2 = 1$), x_3 has 2 branch points (p^2) leading 3 surviving lines ($(1-p)^3$) and two diagrams ($C_3 = 2$), x_4 has 3 branch points (p^3), 4 surviving lines ($(1-p)^4$) and 5 diagrams ($C_4 = 5$), etc. In these evolutionary/ancestral variables the $f_0 = \sum x_k = 2x(1 - \sqrt{1-z})$ which determines Z is $f_0 = \beta$ for all $p \leq 1/2$. For $p \geq 1/2$, $f_0 = \sum x_k$ is no longer a constant and is $f_0 = \beta(1-p)/p$. To keep $f_0 = \sum_k x_k$ a constant without changing $f_1 = \langle n \rangle = \sum_k k \langle n_k \rangle = \beta \frac{(1-p)}{|1-2p|}$, a $x_\infty = \phi_\infty$ was introduced in Ref. [31]. The $\phi_\infty = 0$ for $p \leq 1/2$ and $\phi_\infty = \beta(2p-1)/p$ for $p \geq 1/2$. For $p \geq 1/2$ there is a finite probability ($\phi_\infty \neq 0$) that the splitting will go on forever ($k \rightarrow \infty$). In percolation above a certain p an infinite cluster is formed and ϕ_∞ is similar to the strength of the infinite cluster. Moreover the sudden appearance of ϕ_∞ is similar to the behavior of an order parameter in a phase transition. The appearance of ϕ_∞ can also be interpreted as the sudden appearance of a jet without pion ($k=0$), if we introduce $x_0 = \phi_\infty$ instead of $x_\infty = \phi_\infty$.

Since the clan variables are $N_c = \langle M \rangle = f_0$ and $n_c = \langle A \rangle / N_c = f_1 / f_0$, then, for the LC model with evolutionary or ancestral variables β and p ,

$$\begin{aligned}
N_c = \langle M \rangle = f_0 &= \beta \frac{1 - |1 - 2p|}{2p} \\
n_c = \langle A \rangle / N_c &= \frac{2p(1-p)}{|1-2p|(1-|1-2p|)} \\
\langle A \rangle &= \beta \frac{(1-p)}{|1-2p|} \\
p &= \frac{1}{2} \left[1 \mp \frac{1}{2n_c - 1} \right] \\
\beta &= N_c \frac{n_c - (1 \pm 1)/2}{n_c - 1}
\end{aligned}$$

These can be reduced to $N_c = \beta$, $n_c = (1-p)/(1-2p)$, and $2p = 1 - 1/(2n_c - 1)$ for $p \leq 1/2$ while $N_c = \beta(1-p)/p$, $n_c = p/(2p-1)$, and $2p = 1 + 1/(2n_c - 1)$ for $p > 1/2$. Since the branching probability p varies in $0 \leq p \leq 1$, the clan variable n_c has $n_c \geq 1$ with $n_c = 1$ at $p = 0$ and 1, only one member per clan in average, and $n_c = \infty$ at $p = 1/2$, infinitely many members per clan. The LC model thus connects the clan variable n_c to the probability p of branching in the evolutionary or ancestral picture of Fig.2 or in a percolation model. For Poisson processes $p = 0$ (no branching), $x_k = \beta \delta_{k1}$ (only unit cycles and no BE correlations) and $n_c = 1$ (one member in each clan in average).

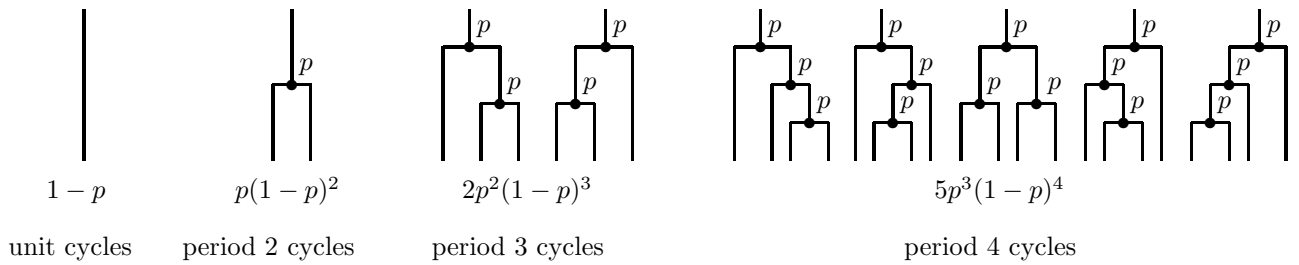


FIG. 2. Evolutionary lines of descent in a hierarchical topology. Each branch increases the cycle length with probability p , survival $1-p$. The probability distribution evolves from Poisson to chaotic. For clusters each branch generates a bigger cluster.

A connection of the LC model can also be made with a Ginzburg-Landau theory of phase transitions and a Feynman-Wilson Gas. These connections are discussed in Ref. [32]. where x and z are related to coefficients in the Ginzburg-Landau approach.

F. Unifying various distributions with Gauss hypergeometric series

Once we identify an appropriate x_k for a physical system, then we may use our general model to study the statistical behavior of the system. The various models used in pion distribution can be related to our general model with $\alpha_k = k$ by choosing x_k as a term in a Gauss hypergeometric series $F(a, b; c; z)$;

$$F(a, b; c; z) = \sum_{m=0}^{\infty} \frac{[a]_m [b]_m z^m}{[c]_m m!} \quad (44)$$

$$[a]_m = \frac{\Gamma(a+m)}{\Gamma(a)} = \frac{\Gamma(a+n)}{\Gamma(a)} \frac{\Gamma(a+n+m-n)}{\Gamma(a+n)} = [a]_n [a+n]_{m-n} \quad (45)$$

Usefull values of $[a]_n$ are $[1/2]_n = (2n)!/(n!2^{2n})$, $[1]_n = n!$, $[2]_n = (n+1)!$. Considering only positive k , we choose

$$x_k = x \frac{[a]_{k-1} [b]_{k-1}}{[c]_{k-1}} \frac{z^k}{(k-1)!} = x \frac{\Gamma(a+k-1)}{\Gamma(a)} \frac{\Gamma(c)}{\Gamma(c+k-1)} \frac{\Gamma(b+k-1)}{\Gamma(b)} \frac{z^k}{(k-1)!} \quad (46)$$

For this case, the thermodynamic grand potential or the generating function is

$$f_0(\vec{x}) = f_0(x, z) = \log Z(x, z) = -\Omega(x, z) = \sum_{k=1}^{\infty} x_k = xzF(a, b; c; z) \quad (47)$$

If we allow jets without a pion, then we may allow $k = 0$ also. For such a case,

$$x_k = x \frac{[a]_k [b]_k z^k}{[c]_k k!} = x \frac{\Gamma(a+k)}{\Gamma(a)} \frac{\Gamma(c)}{\Gamma(c+k)} \frac{\Gamma(b+k)}{\Gamma(b)} \frac{z^k}{k!} \quad (48)$$

$$f_0(\vec{x}) = f_0(x, z) = \log Z(x, z) = -\Omega(x, z) = \sum_{k=0}^{\infty} x_k = xF(a, b; c; z) \quad (49)$$

We can see the only difference of the generating functions between the above two cases is the extra factor z for the grand potential. We will mostly concentrate on the first case, i.e., $k \neq 0$.

Using Eq. (23) or the recurrence relation Eq.(29) and Eqs.(44) – (47),

$$\begin{aligned} f_m(x, z) &= -z^m \left(\frac{d}{dz} \right)^m \Omega(x, z) = z^m \left(\frac{d}{dz} \right)^m \log Z(x, z) = z^m \left(\frac{d}{dz} \right)^m xzF(a, b; c; z) \\ &= x \frac{[a]_m [b]_m}{[c]_m} z^{m+1} F(a+m, b+m; c+m; z) \\ &\quad + xm \frac{[a]_{m-1} [b]_{m-1}}{[c]_{m-1}} z^m F(a+m-1, b+m-1; c+m-1; z) \end{aligned} \quad (50)$$

The second order normalized factorial cumulant $\xi = \kappa_2$ and the void variable χ are then

$$\begin{aligned} \xi(x, z) \langle A \rangle &= \frac{f_2(x, z)}{\langle A \rangle} = \frac{f_2(x, z)}{f_1(x, z)} \\ &= \frac{\frac{[a]_2 [b]_2}{[c]_2} z^2 F(a+2, b+2; c+2; z) + 2 \frac{ab}{c} z F(a+1, b+1; c+1; z)}{\frac{ab}{c} z F(a+1, b+1; c+1; z) + F(a, b; c; z)} \end{aligned} \quad (51)$$

$$\begin{aligned} \chi(x, z) &= \frac{f_0(x, z)}{\langle A \rangle} = \frac{f_0(x, z)}{f_1(x, z)} \\ &= \frac{F(a, b; c; z)}{\frac{ab}{c} z F(a+1, b+1; c+1; z) + F(a, b; c; z)} \end{aligned} \quad (52)$$

For some values of a , b , and c , the hypergeometric function become a simple function;

$$\begin{aligned}
F(a, b; b; z) &= (1 - z)^{-a} \\
F(a, b; a; z) &= (1 - z)^{-b} \\
F(a, 1; 2; z) &= \frac{1 - (1 - z)^{1-a}}{z(1 - a)} \\
F(1, 1; 2; z) &= \lim_{a \rightarrow 1} F(a, 1; 2; z) = -\frac{\ln(1 - z)}{z}
\end{aligned} \tag{53}$$

Various models of pion distributions can be related with these functions as listed in Table I.

TABLE I. Various models with specific choice of $\alpha_k = k$ and x_k in hypergeometric series $F(a, b; c; z)$ of Eq.(44). Here $k = 0$ is not included, and thus $f_0 = \ln Z = \sum_{k=1}^{\infty} x_k = xzF(a, b; c; z)$. Here $1 \leq k \leq N$ with $N \rightarrow \infty$ except for Poisson which has a finite Nx . Fisher exponent τ for each x_k as discussed in Sect.II C are given too.

Model	x_k	$f_0(\bar{x}) = \ln Z$	a	b	c	τ
Poisson (P)	$Nx\delta_{k,1}$ or x for $k = 1, 2, \dots, N$	$Nx = A$				
Geometric (Geo)	xz^k	$\frac{xz}{1-z}$	a	1	a	0
Negative Binomial (NB)	$\frac{1}{k}xz^k$	$-x \ln(1 - z)$	1	1	2	1
Signal/Noise (SN)	$(y + \frac{x}{k})z^k$	$\frac{yz}{1-z} - x \ln(1 - z)$				
Lorentz/Catalan (LC)	$\frac{1}{k}2^{-2(k-1)} \binom{2(k-1)}{k-1} xz^k$	$2x[1 - (1 - z)^{1/2}]$	$\frac{1}{2}$	1	2	3/2
Hypergeometric (HGa)	$\frac{[a]_{k-1}}{k!} xz^k$	$\frac{x}{1-a}[1 - (1 - z)^{1-a}]$	a	1	2	$2 - a$
Random Walk-1d (RW1D)	$2^{-2(k-1)} \binom{2(k-1)}{k-1} xz^k$	$xz(1 - z)^{-1/2}$	$\frac{1}{2}$	1(b)	1(b)	1/2
Random Walk-2d (RW2D)	$\left[2^{-2(k-1)} \binom{2(k-1)}{k-1}\right]^2 xz^k$	$xzF(\frac{1}{2}, \frac{1}{2}; 1; z)$	$\frac{1}{2}$	$\frac{1}{2}$	1	1
Generalized RW1D (GRW1D)	$\frac{[a]_{k-1}}{(k-1)!} xz^k$	$xz(1 - z)^{-a}$	a	b	b	$1 - a$
Generalized RW2D (GRW2D)	$\left[\frac{[a]_{k-1}}{(k-1)!}\right]^2 xz^k$	$xzF(a, a; 1; z)$	a	a	1	$2(1 - a)$

TABLE II. Factorial cumulants for various choices of x_k of Table.I

Model	$f_0 = \log Z$	$f_1 = \langle A \rangle$	$z^{-2}f_2$	$z^{-m}f_m$
P	$Nx = A$	A	0	0 for $m \geq 2$
Geo	$x \frac{z}{1-z}$	$x \frac{z}{(1-z)^2}$	$x \frac{2}{(1-z)^3}$	$x \frac{m!}{(1-z)^{m+1}}$
NB	$-x \ln(1 - z)$	$x \frac{z}{1-z}$	$x \frac{1}{(1-z)^2}$	$x \frac{(m-1)!}{(1-z)^m}$
SN	$\frac{yz}{1-z} - x \ln(1 - z)$	$y \frac{z}{(1-z)^2} + x \frac{z}{1-z}$	$y \frac{2}{(1-z)^3} + x \frac{1}{(1-z)^2}$	$\frac{(m-1)!}{(1-z)^m} \left(y \frac{m}{(1-z)} + x \right)$
LC	$2x[1 - (1 - z)^{1/2}]$	$x \frac{z}{(1-z)^{1/2}}$	$x \frac{1/2}{(1-z)^{3/2}}$	$x \frac{[1/2]_m}{(1-z)^{m-1/2}}$
HGa	$\frac{x}{1-a}[1 - (1 - z)^{1-a}]$	$x \frac{z}{(1-z)^a}$	$x \frac{a}{(1-z)^{a+1}}$	$x \frac{[a]_{m-1}}{(1-z)^{a+m-1}}$
RW1D	$x \frac{z}{(1-z)^{1/2}}$	$\frac{x}{2} \frac{z}{(1-z)^{1/2}} + \frac{x}{2} \frac{z}{(1-z)^{3/2}}$	$\frac{x}{4} \frac{1}{(1-z)^{3/2}} + \frac{3}{4} x \frac{1}{(1-z)^{5/2}}$	$-x \frac{[-1/2]_m}{(1-z)^{a+1}} + x \frac{[1/2]_m}{(1-z)^{a+2}}$
GRW1D	$x \frac{z}{(1-z)^a}$	$-x \frac{(a-1)z}{(1-z)^a} + x \frac{az}{(1-z)^{a+1}}$	$-x \frac{(a-1)a}{(1-z)^{a+1}} + x \frac{a(a+1)}{(1-z)^{a+2}}$	$-x \frac{[a-1]_m}{(1-z)^{a+m-1}} + x \frac{[a]_m}{(1-z)^{a+m}}$

More detail discussions and related physical systems of these distributions will be given and discussed in the next section. Brief discussion about the weight x_k of each model follows. All the distributions, except the Poisson distribution (P), considered in Table I have several factors in the weight x_k . One factor in x_k is z^k which is a k dependent geometric term and comes from assigning the same weight z to each constituents independent of the cluster or cycle classes it belongs to. Another factor of weight is independent of k such as the x in Table I which comes from assigning the same weight x to each cluster or the cycle class as a whole independent of its internal structure. These two factors, xz^k , are multiplied by a k dependent or independent prefactor. A geometric (Geo) distribution follows when there is no other weight factor beside x and z , i.e., no k dependent prefactor so that $x_k = xz^k$. The Geo with $z = 1$ for a finite N and with $z = 0$ for $k > N$ is the same as the Poisson distribution; both have $f_0 = Nx$. The negative binomial (NB) which appears frequently in various studies has a weight factor assigned to a cluster or cycle class given by xz^k/k . This has an extra size dependent factor of $1/k$ compared to the geometric distribution. The signal/noise model (SN) has a two part structure and interpolates between a Poisson and NB distribution. The geometric distribution is the signal component of SN while the NB distribution is the noise component of SN. The Lorentz/Catalan model (LC) has in its weight a shifted Catalan number divided by $2^{2(k-1)}$, that is $\frac{[1/2]_{k-1}}{k!} = \frac{2^{-2(k-1)}}{k} \binom{2(k-1)}{k-1}$, beside the xz^k factor which is the weight for Geo model. The Catalan numbers given by $\binom{2k}{k}/(k+1)$ are 1, 2, 5, 14, \dots for $k = 1, 2, 3, 4, \dots$ and the shifted Catalan numbers given by $\binom{2(k-1)}{k-1}/k$ are 1, 1, 2, 5, 14, \dots . The importance of this factor is shown in Fig. 2 of section II E.

Of all these distributions, the NB has been the most frequently studied. Ref. [33] gives several sources for its origin. These sources include sequential processes, self-similar cascade models and connections with Cantor sets and fractal structure, generalizations of the Planck distribution, solutions to stochastic differential equations. Becattini [34] have shown that the NB distribution arises from decaying resonances. The α model of Ref. [8], which is a self similar random cascade process, leads to a NB like behavior. The stochastic aspects of the NB distribution have been discussed by R. Hwa [35]. Hegyi [36] has discussed the NB distribution in terms of combinatorics. As already mentioned, the LC model can be connected to a Ginzburg-Landau approach and also has an underlying splitting or branching dynamics and cascade like features.

As can be seen from the arguments of the hypergeometric function $F(a, b; c; z)$ in Table I, the hypergeometric model with $b = 1$ and $c = 2$ (HGa) include Geo, NB, SN, LC as a special case of HGa depending on the value of a . Other models listed in Table I are based on random walks. The use of random walk results was originally due to Feynman [37] in his description of the phase transition in liquid helium. The random walk aspects arise when considering the closing of cycle of length k . We include them for completeness. Since the random walk in 1-dimension (RW1D) is the same as LC except the missing $1/k$ dependence compared to LC, RW1D can be extended to a generalized RW1D (GRW1D) similar to the generalization of LC to HGa. A random walk model in 2-dimension has an extra factor of a shifted Catalan number and $k2^{-2(k-1)}$ factor compared to RW1D and can also be generalized to GRW2D.

Since $k = 0$ is excluded here, the partition function for these models are given simply by a hypergeometric function as $Z = \exp[\sum_{k=1}^{\infty} x_k] = \exp[xzF(a, b; c; z)]$ with various choices of a, b, c . For example the LC model has $f_0 = \sum_k x_k = xzF(1/2, 1; 2; z)$ and the NB model has $f_0 = xzF(1, 1; 2; z)$. The geometric model $x_k = yz^k$ has $f_0 = yzF(a, 1; a; z) = yzF(2, 1; 2; z)$ while the SN model is a combination of the geometric plus NB cases. These functions are special cases of $f_0 = xzF(a, 1; 2; z)$ of the HGa model. The generalized random work in 1-dimension (GRW1D) has $f_0 = xzF(a, b; b; z)$ and the generalization of RW in 2-dimension (GRW2D) has $f_0 = xzF(a, a; 1; z)$. The factorial cumulants f_m for these models are summarized in Table II. Several cases with $c = 2$ have a canonical partition function Z_n which can be written in terms of confluent hypergeometric functions $U(u, v; w)$ and standard factor $z^n/n!$ [32].

G. Generalized model of Hypergeometric (HGa)

We consider in more detail the hypergeometric model with $b = 1$ and $c = 2$ (HGa) here since it includes the NB, Geo, and LC models as special cases. This generalized model is related with the hypergeometric function with $b = 1$ and $c = 2$ with an arbitrary value of a , i.e., $F(a, 1; 2; z)$, and has the weight of

$$x_k = xz^k \frac{[a]_{k-1}}{k!} = x \frac{z^k}{k!} \frac{\Gamma(a+k-1)}{\Gamma(a)} \quad (54)$$

The asymptotic behavior of x_k is

$$x_k = xz^k k^{a-2}/\Gamma(a) = xz^k k^{-\tau}/\Gamma(a) \quad (55)$$

for large k using Stirling approximation. Thus

$$\tau = 2 - a \quad (56)$$

which connects the parameter a to the physical Fisher critical exponent τ for the HGa class of distributions. Its associated grand canonical partition function

$$Z(x, z) = e^{f_0} = e^{xzF(a,1;2;z)} = \exp \left[\frac{x}{(a-1)} \left(\frac{1}{(1-z)^{(a-1)}} - 1 \right) \right] \quad (57)$$

is shown in Table I. From Table II, we have

$$f_m(x, z) = [a]_{m-1} \frac{xz^m}{(1-z)^{a+m-1}} = x \frac{\Gamma(a+m-1)}{\Gamma(a)} \frac{z^m}{(1-z)^{a+m-1}} \quad (58)$$

$$\begin{aligned} \kappa_m(x, z) &= \frac{[a]_{m-1}}{x^{m-1}} (1-z)^{(a-1)(m-1)} = \frac{\Gamma(a+m-1)}{\Gamma(a)} \left(\frac{(1-z)^{(a-1)}}{x} \right)^{m-1} \\ &= \frac{\Gamma(a+m-1)}{\Gamma(a)} \frac{\kappa_2^{m-1}(x, z)}{a^{m-1}} = A_m \kappa_2^{m-1}(x, z) \end{aligned} \quad (59)$$

The normalized factorial cumulant, i.e., the reduced cumulant κ_m shows the hierarchical structure of HGa at the reduced cumulant level with $A_m = a^{-(m-1)}\Gamma(a+m-1)/\Gamma(a)$ where κ_m is related to κ_2 . This property was realized for the NB distribution in Ref. [28] which is obtained for Eq.(59) with $a = 1$ giving $A_m = (m-1)!$. The result of Eq.(59) is a generalization of the NB result.

Some moments for HGa are

$$\langle A \rangle(x, z) = f_1(z, \vec{x}) = \frac{xz}{(1-z)^a} \quad (60)$$

$$\chi(x, z) = \frac{f_0(x, z)}{f_1(x, z)} = \frac{1}{(1-a)} \frac{(1-z)}{z} [(1-z)^{a-1} - 1] \quad (61)$$

$$\xi(x, z) = \kappa_2(x, z) = \frac{f_2(x, z)}{f_1^2(x, z)} = \frac{a}{x} (1-z)^{(a-1)} \quad (62)$$

Since these relations give

$$\xi(x, z) \langle A \rangle(x, z) = \kappa_2(x, z) \langle A \rangle(x, z) = \frac{f_2(x, z)}{f_1(x, z)} = \frac{az}{(1-z)} \quad (63)$$

the void parameters can be obtained in terms of the normalized fluctuation ξ and the mean number $\langle A \rangle = \bar{A}$ by

$$z(\bar{A}, \xi) = \frac{\xi \bar{A}}{a + \xi \bar{A}} = \frac{f_2/\bar{A}}{a + f_2/\bar{A}} = \frac{f_2}{f_2 + a\bar{A}} \quad (64)$$

$$x(\bar{A}, \xi) = \frac{\bar{A}}{z} (1-z)^a = \frac{a}{\xi} \left(\frac{a}{a + \xi \bar{A}} \right)^{(a-1)} = \frac{a\bar{A}^2}{f_2} \left(\frac{a\bar{A}}{a\bar{A} + f_2} \right)^{a-1} \quad (65)$$

$$f_0(\bar{A}, \xi) = \log Z(\bar{A}, \xi) = \frac{x}{a-1} \left[\left(1 + \frac{\xi \bar{A}}{a} \right)^{a-1} - 1 \right] = \frac{x}{a-1} \left[\left(1 + \frac{f_2}{a\bar{A}} \right)^{a-1} - 1 \right] \quad (66)$$

$$\chi(\bar{A}, \xi) = \frac{f_0}{\bar{A}} = \frac{1}{(1-a)} \frac{a}{\xi \bar{A}} \left[\left(1 + \frac{\xi \bar{A}}{a} \right)^{1-a} - 1 \right] = \frac{1}{(1-a)} \frac{a\bar{A}}{f_2} \left[\left(1 + \frac{f_2}{a\bar{A}} \right)^{1-a} - 1 \right] \quad (67)$$

$$\kappa_m(\bar{A}, \xi) = \frac{f_m(\bar{A}, \xi)}{\bar{A}^m} = \frac{\Gamma(a+m-1)}{\Gamma(a)} \left(\frac{\xi}{a} \right)^{m-1} \quad (68)$$

for a given mean value of $\langle A \rangle = \bar{A}$ and the fluctuation ξ or $\xi \bar{A}$ or f_2 . Using these $x(\bar{A}, \xi)$ and $z(\bar{A}, \xi)$ we can easily find the multiparticle distribution $P_A(\bar{A}, \xi)$ for a given values of mean \bar{A} and fluctuation ξ using the recurrence relation

of Eq.(6) for $Z_A(\bar{A}, \xi)$. We explicitly compare the distribution P_A for different values of a with given values of \bar{A} and ξ in Sect.III.

Table I shows that the generalized HGa model becomes the Lorentz/Catalan (LC) model with $a = 1/2$, the negative binomial (NB) model with $a = 1$, and geometric (Geo) distribution with $a = 2$. However the NB should be considered as a $a \rightarrow 1$ limit of HGa;

$$\lim_{a \rightarrow 1} f_0 = -x \log(1 - z) \quad (69)$$

$$\lim_{a \rightarrow 1} Z = (1 - z)^{-x} \quad (70)$$

$$\lim_{a \rightarrow 1} f_0(\bar{A}, \xi) = x \ln(1 + \xi \bar{A}) = x \ln(1 + f_2/\bar{A}) \quad (71)$$

$$\lim_{a \rightarrow 1} \chi(\bar{A}, \xi) = \frac{1}{\xi \bar{A}} \log(1 + \xi \bar{A}) \quad (72)$$

Thus a NB distribution has $\chi = \ln(1 + \xi \bar{A})/(\xi \bar{A})$ with $x = 1/\xi$ while the LC distribution has $\chi = (\sqrt{1 + 2\xi \bar{A}} - 1)/(\xi \bar{A})$ with $x = \sqrt{1 + 2\xi \bar{A}}/(2\xi)$ and a Geo distribution has $\chi = 2[1 - (1 + \xi \bar{A}/2)^{-1}]/(\xi \bar{A})$ with $1/x = \xi(1 + \xi \bar{A}/2)/2$ as limiting expressions of a more general χ given by Eq.(67) for HGa. Eq.(65) shows that the fluctuation ξ depends on the mean \bar{A} for given x except for NB. Since $\xi \geq 0$ for $\alpha_k = k$ with non-negative x_k , $\xi(\bar{A}, x) = 1/x$ for $a = 1$ (NB), $\xi(\bar{A}, x) = [\bar{A} + \sqrt{\bar{A}^2 + 4x^2}]/(4x^2)$ for $a = 1/2$ (LC), $\xi(\bar{A}, x) = [-x + \sqrt{x^2 + 4x\bar{A}}]/(x\bar{A})$ for $a = 2$ (Geo). However for small \bar{A} and large x the fluctuation ξ is independent of the mean \bar{A} and $\xi(\bar{A}, x) \approx a/x$ for HGa.

The void parameters are $\xi = 0$ and $\chi = 1$ for Poisson distribution. The reduced cumulants are $\kappa_m = 0$ for $m > 2$ for Poisson distribution. The void parameters are $\xi = \frac{1}{x}$ and $\chi = \frac{\ln(1 + \xi \bar{A})}{\xi \bar{A}}$ for NB distribution. The m -th order reduced cumulant is $\kappa_m = (m - 1)! \xi^{m-1}$ for NB. For SN distribution, the void parameters are

$$\xi = \frac{f_2}{f_1^2} = \frac{N(2S + N)}{x(S + N)^2} \quad (73)$$

$$\chi = \frac{f_0}{f_1} = \frac{x \ln(1 + N/x) + S/(1 + N/x)}{S + N} \quad (74)$$

with signal level $S = \frac{yz}{(1-z)^2}$ and noise level $N = \frac{xz}{1-z}$. The SN model has important application to quantum optics and, in particular, to photon counts from lasers [38]. Biyajima [39] has suggested using it for particle multiplicity distribution as does Ref. [33]. When the noise level $N \rightarrow 0$, $\xi \rightarrow 0$ and $\chi \rightarrow 1$. When the signal level $S \rightarrow 0$, $\xi \rightarrow 1/x$ and $\chi \rightarrow \frac{x}{N} \ln(1 + N/x)$. The third order reduced cumulant is $\kappa_3 = \frac{2!}{(1-z)^3} \left(\frac{3y}{(1-z)} + x \right) = 2 \frac{x}{N} (1 + N/x)^3 (3S + N)$ for SN. For LC distribution, the void parameters are $\xi = \frac{1}{2x\sqrt{1-z}}$ and $\chi = \frac{1}{\xi \bar{A}} \left[\sqrt{1 + 2\xi \bar{A}} - 1 \right]$ with $z = 2\xi \bar{A}/(1 + 2\xi \bar{A})$. The m -th order reduced cumulant is $\kappa_m = \left[\frac{1}{2} \right]_{m-1} (2\xi)^{m-1}$ for LC. The results of quantum optics, in the notation of Ref. [38], can be obtained [31] when $x = T\Omega/2$, $z = 2W\gamma/\Omega^2$, $\Omega^2 = \gamma^2 + 2W\gamma$. The W is an integral of the Lorentzian line shape $\Gamma(\omega) = b/[(\omega - \omega_0)^2 + \gamma^2]$, T is the time, and $2x\sqrt{1-z} = \gamma T$.

H. Generalized random walk in one dimension

The hypergeometric model with $c = b$ has $x_k = x \frac{[a]_{k-1}}{(k-1)!} z^k$ which is a generalized random walk process in one dimension (GRW1D). For $a = 1/2$ the GRW1D becomes the random walk in one dimension. Since $F(a, b; c; z) = F(b, a; c; z)$, it is easy to see that both HGa with $a = 2$ and GRW1D with $a = 1$ are geometric models. For GRW1D, we have $f_0 = x \frac{z}{(1-z)^a}$ which is f_1 of HGa as shown in Table II. The asymptotic behavior of $x_k = x \frac{[a]_{k-1}}{(k-1)!} z^k$ is $x_k = x z^k k^{a-1}/\Gamma(a)$ for large k and thus the Fisher critical exponent is $\tau = 1 - a$ for the GRW1D class of distributions. Its associated grand canonical partition function is

$$Z(x, z) = e^{f_0} = e^{x z F(a, b; b; z)} = \exp \left[\frac{xz}{(1-z)^a} \right] \quad (75)$$

The factorial cumurants for GRW1D are, from Table II,

$$f_m(x, z) = -x \frac{[a-1]_m}{(1-z)^{a+m-1}} z^m + x \frac{[a]_m}{(1-z)^{a+m}} z^m$$

$$= x [a]_{m-1} \frac{[(a-1)z+m]}{(1-z)^{a+m}} z^m \quad (76)$$

$$\begin{aligned} \kappa_m(x, z) &= x \frac{[a]_{m-1} z^m}{(1-z)^{a+m}} [(a-1)z+m] \left[x \frac{z}{(1-z)^{a+1}} \right]^{-m} [(a-1)z+1]^{-m} \\ &= \left[\frac{(1-z)^a}{x [(a-1)z+1]} \right]^{m-1} \frac{[a]_{m-1} [(a-1)z+m]}{[(a-1)z+1]} \\ &= [a+1]_{m-2} \frac{[(a-1)z+m]}{[(a-1)z+2]} \left[\frac{[(a-1)z+1]}{a[(a-1)z+2]} \right]^{m-2} \kappa_2^{m-1} = A_m \kappa_2^{m-1} \end{aligned} \quad (77)$$

Here the coefficient A_m that appears in the hierarchical structure relation of Eq.(77) depends also on z which means that A_m depends on the mean \bar{A} and the normalized fluctuation ξ . For HGa A_m is independent of \bar{A} and ξ .

Some moments for GRW1D are

$$\langle A \rangle(x, z) = \bar{A} = f_1(x, z) = \frac{xz}{(1-z)^{a+1}} [(a-1)z+1] \quad (78)$$

$$\chi(x, z) = \frac{f_0(x, z)}{f_1(x, z)} = \frac{(1-z)}{[(a-1)z+1]} \quad (79)$$

$$\xi(x, z) = \kappa_2(x, z) = \frac{f_2(x, z)}{f_1^2(x, z)} = \frac{a}{x} (1-z)^a \frac{[(a-1)z+2]}{[(a-1)z+1]^2} \quad (80)$$

Since these gives

$$\xi(x, z) \langle A \rangle(x, z) = \kappa_2(x, z) \langle A \rangle(x, z) = \frac{f_2(x, z)}{f_1(x, z)} = \frac{az}{(1-z)} \frac{[(a-1)z+2]}{[(a-1)z+1]} \quad (81)$$

we have, for a given mean value $\langle A \rangle = \bar{A}$ and the fluctuation ξ or f_2 ,

$$z(\bar{A}, \xi) = \frac{(a-2)\xi\bar{A} - 2a \pm a\sqrt{(\xi\bar{A})^2 + 4\xi\bar{A}/a + 4}}{2(a-1)(\xi\bar{A} + a)} \xrightarrow{a \rightarrow 1} \frac{\xi\bar{A}}{2 + \xi\bar{A}} \quad (82)$$

$$\begin{aligned} x(\bar{A}, \xi) &= \frac{\bar{A}}{z} \frac{(1-z)^{a+1}}{[(a-1)z+1]} \\ &= \frac{\bar{A}}{z} \left(\frac{2(\xi\bar{A} + a)}{a\xi\bar{A} \pm a\sqrt{(\xi\bar{A})^2 + 4\xi\bar{A}/a + 4}} \right) \left(\frac{a\xi\bar{A} + 2a^2 \mp a\sqrt{(\xi\bar{A})^2 + 4\xi\bar{A}/a + 4}}{2(a-1)(\xi\bar{A} + a)} \right)^{a+1} \end{aligned} \quad (83)$$

$$f_0(\bar{A}, \xi) = x \frac{z}{(1-z)^a} = xz \left(\frac{2(a-1)(\xi\bar{A} + a)}{a\xi\bar{A} + 2a^2 \mp a\sqrt{(\xi\bar{A})^2 + 4\xi\bar{A}/a + 4}} \right)^a \quad (84)$$

$$\chi(\bar{A}, \xi) = \frac{f_0}{\bar{A}} = \left(\frac{\xi\bar{A} + 2a \mp \sqrt{(\xi\bar{A})^2 + 4\xi\bar{A}/a + 4}}{\xi\bar{A} \pm \sqrt{(\xi\bar{A})^2 + 4\xi\bar{A}/a + 4}} \right) \frac{1}{(a-1)} \xrightarrow{a \rightarrow 1} \frac{2}{2 + \xi\bar{A}} \quad (85)$$

$$\begin{aligned} \kappa_m(\bar{A}, \xi) &= \frac{f_m(\bar{A}, \xi)}{\bar{A}^m} = [a]_{m-1} \left[\frac{(a-1)z+m}{(a-1)z+2} \right] \left[\frac{(a-1)z+1}{(a-1)z+2} \right]^{m-2} \left(\frac{\kappa_2}{a} \right)^{m-1} \\ &= \left(\frac{(a+2(m-1))\xi\bar{A} + 2(m-1)a \pm a\sqrt{(\xi\bar{A})^2 + 4\xi\bar{A}/a + 4}}{(a+2)\xi\bar{A} + 2a \pm a\sqrt{(\xi\bar{A})^2 + 4\xi\bar{A}/a + 4}} \right) \\ &\quad \times \left(\frac{a\xi\bar{A} \pm a\sqrt{(\xi\bar{A})^2 + 4\xi\bar{A}/a + 4}}{(a+2)\xi\bar{A} + 2a \pm a\sqrt{(\xi\bar{A})^2 + 4\xi\bar{A}/a + 4}} \right)^{m-2} [a]_{m-1} \left(\frac{\xi}{a} \right)^{m-1} \end{aligned} \quad (86)$$

Here the condition $0 < z < 1$ determines the right one of \pm sign. Note here that $\kappa_m(\bar{A}, \xi) = [a]_{m-1} \left(\frac{\xi}{a} \right)^{m-1}$ for HGa. For the GRW1D, the normalized factorial cumulant $\kappa_m(\bar{A}, \xi)$ has an extra dependence of the order m which also depends on the mean \bar{A} and the fluctuation ξ .

III. COMPARISON OF PROBABILITY DISTRIBUTIONS WITHIN HGA

The hypergeometric case (HGa) which we studied in more detail in Sect. II G included various cases of Table I; Geo, NB, LC which are distinguished by one parameter a of the hypergeometric model. Thus we use HGa to compare various models for pion distribution and other particle distributions, with particle number $n = \sum_k kn_k$.

A. Voids and void scaling relations

Void analysis looks for scaling properties associated with $\chi = f_0/\langle n \rangle$; specifically, χ is a function of the combination $\xi\langle n \rangle = f_2/\langle n \rangle$ where $\xi = \kappa_2$ is the coefficient of $\langle n \rangle^2$ in the fluctuation $\sigma^2 = \langle n^2 \rangle - \langle n \rangle^2 = \langle n \rangle + \xi\langle n \rangle^2$. For generalized HGa model χ is given by

$$\chi = \frac{(1 + \xi\langle n \rangle/a)^{1-a} - 1}{(1-a)\xi\langle n \rangle/a} \quad (87)$$

We show the void variable χ as a function of $\xi\langle n \rangle$ in Fig.3. This shows that we can vary a to fit data. Ref. [28] claims the NB distribution (HGa with $a = 1$) fits reasonably well the void distribution for single jet events in e^+e^- annihilation but Fig.3 shows all of the curves might fit such data up to $\xi\langle n \rangle \sim 1$ since the various curves are reasonably close up to this $\xi\langle n \rangle$. Thus further investigations of this data is required to distinguish various models. Higher moments or cumulants might need to be compared for this purpose. Within HGa, $\kappa_3(\bar{n}, \xi, a) = \left(\frac{a+1}{a}\right) \xi^2$ for a given value of $\langle n \rangle = \bar{n}$ and ξ according to Eq.(68). Thus $A_3 = \kappa_3/\xi^2 = (a+1)/a = 3, 2, 3/2, 4/3, 5/4$ for $a = 1/2, 1, 2, 3, 4$ independent of ξ . The κ_3 may help in distinguishing various models for the data with a small value of ξ , i.e., the region of $\xi\bar{n} < 1$ in Fig.3. The differences of A_m between models with different value of a becomes larger as the order m of the reduced factorial cummulant becomes higher.

Table III shows the values of ξ and κ_3 of charged particle multiplicity distribution of jets for L3 data [40] and H1 data [41]. From these values $A_3 = 4.1686$ and -6.2653 for L3 and H1 respectively. The corresponding values of HGa model parameter a are 0.31559 and -0.13764 respectively and the corresponding values of GRW1D model parameter a are 0.14006 and -0.8516 . The negative value of a makes the corresponding z value in HGa larger than 1 which is not allowed because of Eq.(65) for real x . Thus the HGa model cannot fit H1 data with the same values of mean, fluctuation and κ_3 at the same time. The negative value of κ_3 or A_3 causes the negative values of a , x and z in GRW1D which are acceptable in Eq.(83) for real x . This model with $a = -0.8516$ fits H1 data best for all the values of mean, fluctuation, κ_3 , and $\chi = f_0/f_1$. The Fisher exponent for this parameter is $\tau = 1 - a = 1.85$. The physical meaning of the negative x and z should be studied further similar as studied in Ref. [21]. Both HGa and GRW1D models with small values of a (0.31559 and 0.14006 respectively) fit the L3 data well with the same mean, fluctuation, and the third cumulant at the same time. The corresponding values of Fisher exponents are $\tau = 2 - a = 1.68$ and $\tau = 1 - a = 0.86$ respectively. If we can extract the value of τ from data then we may distinguish which model fits the data better.

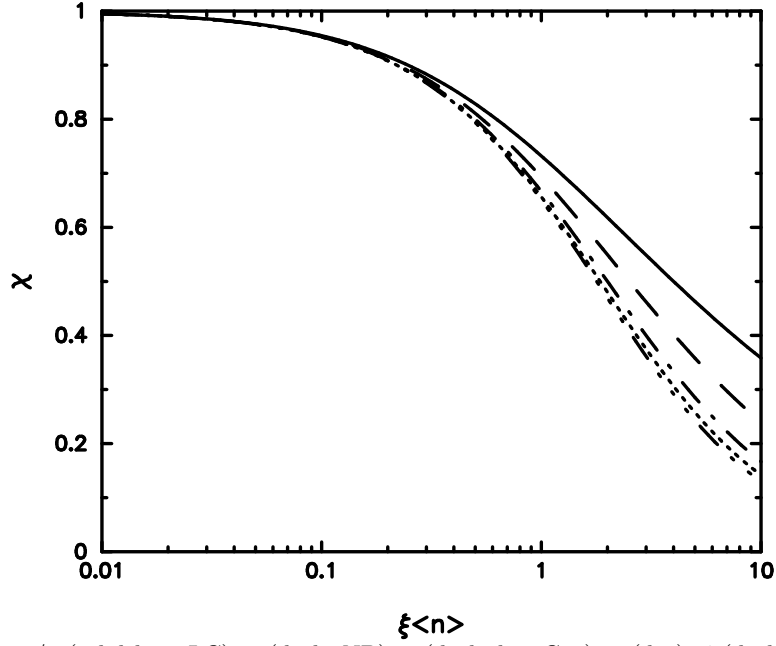


FIG. 3. χ vs $\xi\langle n \rangle$ for $a = 1/2$ (solid line; LC), 1 (dash; NB), 2 (dash-dot; Geo), 3 (dot), 4 (dash-dot-dot-dot). For Poisson distribution $\xi = 0$ and $\chi = 1$.

TABLE III. Various cumulants of charged particle multiplicity distribution of jets for L3 data (all events of e^+e^-) [40] and H1 data (pseudorapidity range $1 < \eta^* < 5$ with $80 \text{ GeV} < W < 115 \text{ GeV}$ of e^+p) [41] compared with models having the same mean and fluctuation.

model	a	x	z	$\langle n \rangle$	ξ	κ_3	χ
L3 data				20.463	0.044238	0.008158	
HGa	0.5 (LC)	18.948	0.64419	20.463	0.044238	0.005871	0.74726
	1.0 (NB)	22.605	0.47514	20.464	0.044238	0.003914	0.71208
	2.0 (Geo)	31.123	0.31159	20.463	0.044238	0.002936	0.68841
	0.31559	18.007	0.74150	20.463	0.044238	0.008158	0.77636
GRW1D	0.14006	20.905	0.66088	20.463	0.044239	0.008158	0.78558
H1 data				7.7210	0.069186	-0.000764	0.73242
HGa	0.5 (LC)	10.394	0.51653	7.7210	0.069186	0.014360	0.82028
	1.0 (NB)	14.454	0.34819	7.7210	0.069186	0.009573	0.80122
	2.0 (Geo)	22.814	0.21079	7.7210	0.069186	0.007180	0.78921
	3.0	31.244	0.15115	7.7210	0.069186	0.006382	0.78470
GRW1D	-0.85160	-4.4150	-0.81168	7.7211	0.069185	-0.000764	0.72375

B. Probability distribution

Once we know the generating function $Z(\vec{x})$ or $f_0(\vec{x})$ we may study the probability distribution P_n using Eq.(9) or the recurrence relation Eq.(6);

$$P_n(x, z) = \frac{Z_n(x, z)}{Z(x, z)} = \frac{1}{Z(x, z)} \frac{z^n}{n!} \left[\left(\frac{d}{dz} \right)^n Z(x, z) \right]_{z=0} \quad (88)$$

for $n = \sum_k kn_k$. For NB which is a special case of HGa in the $a \rightarrow 1$ limit, $x_k = x \frac{z^k}{k}$,

$$Z^{\text{NB}}(x, z) = (1 - z)^{-x} = P_0^{-1}(x, z) \quad (89)$$

$$P_n^{\text{NB}}(x, z) = \frac{1}{Z} \frac{z^n}{n!} \frac{\Gamma(x + n)}{\Gamma(x)} = (1 - z)^x \frac{z^n}{n!} \frac{\Gamma(x + n)}{\Gamma(x)} \quad (90)$$

The P_n for various cases of Table I are shown in Fig.4 and Fig.5 with the same mean value $\langle n \rangle = \bar{n}$ and the same fluctuation $\xi = \kappa_2 = f_2/\bar{n}^2$ for fixed $\langle n \rangle = 10$. Fig.6 shows KNO plots of $\langle n \rangle P_n$ versus $n/\langle n \rangle$ for fixed $\langle n \rangle = 10$ and 20. Fig.4 shows that the various models considered here have almost the same distribution for small fluctuation ($\xi = 0.01$) and in this case they are very similar to a Poisson's distribution. For $\xi = 0.05$ the models are similar to each other except for larger n/\bar{n} even though they are different from a Poisson distribution. For larger fluctuations such as $\xi = 0.5$, the models have very different forms even if they have the same mean value and fluctuation. Fig.5 shows that the probability distribution of these models differ in their form for fluctuations larger than $\xi \approx 0.2$. Ref. [33] shows the total charge distribution in hadronic collisions. They fit the data in the range of $\bar{n} = 6 \sim 13$ using a SN distribution. The SN is a mixture of NB ($a = 1$) and geometric ($a = 2$) which are the cases we have shown in the figures. To determine which model fits the data best, we need to know the exact value of ξ and even higher moments of the data beside the mean value \bar{n} .

Fig.7 shows the multiplicity distribution for L3 data and H1 data discussed in Table III. This shows that all the models having the same mean and fluctuation also have very similar fits to the data for $n/\langle n \rangle$ smaller than 2. For $n/\langle n \rangle$ larger than 2, the NB (thin solid curve) or LC (thick dashed curve) fits best the L3 data. But for $n/\langle n \rangle$ smaller than 1, the GRW1D (thick solid curve) and HGa with $a = 0.31559$ (dash-dotted curve) fit the L3 data best and only these two cases give the correct value of κ_3 for L3. We can also see that the GRW1D (thick solid curves) fits best the H1 data for whole range of $n/\langle n \rangle$. Only this GRW1D model fits the value of κ_3 for H1 data correctly. Thus we need to evaluate higher order moments of data (or at least up to third order, κ_3) beside the mean and fluctuation to understand the distribution of data and its underlying mechanism. One difference between L3 and H1 data is that the H1 data has much larger probability for small $n/\langle n \rangle$ compared to the L3 data. This large probability at small $n/\langle n \rangle$ causes the negative value for the third cumulant κ_3 for the H1 data.

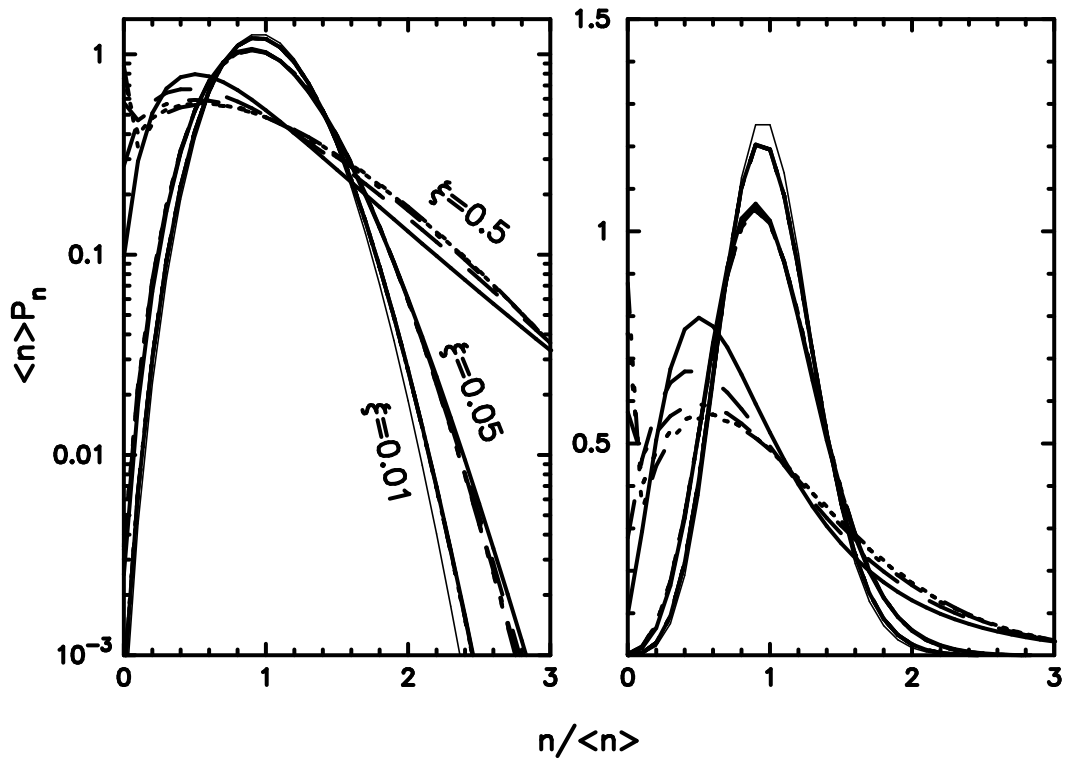


FIG. 4. P_n for fixed $\langle n \rangle = 10$ for $a = 1/2$ (solid line), 1 (dash), 2 (dash-dot), 3 (dot), 4 (dash-dot-dot-dot) and for $\xi = 0.01$, 0.05, and 0.5 in log scale on the left and linear scale on the right. For $\xi = 0.01$ all distributions become very close to Poisson (thin solid curve) already. (P_0 becomes large for large ξ .)

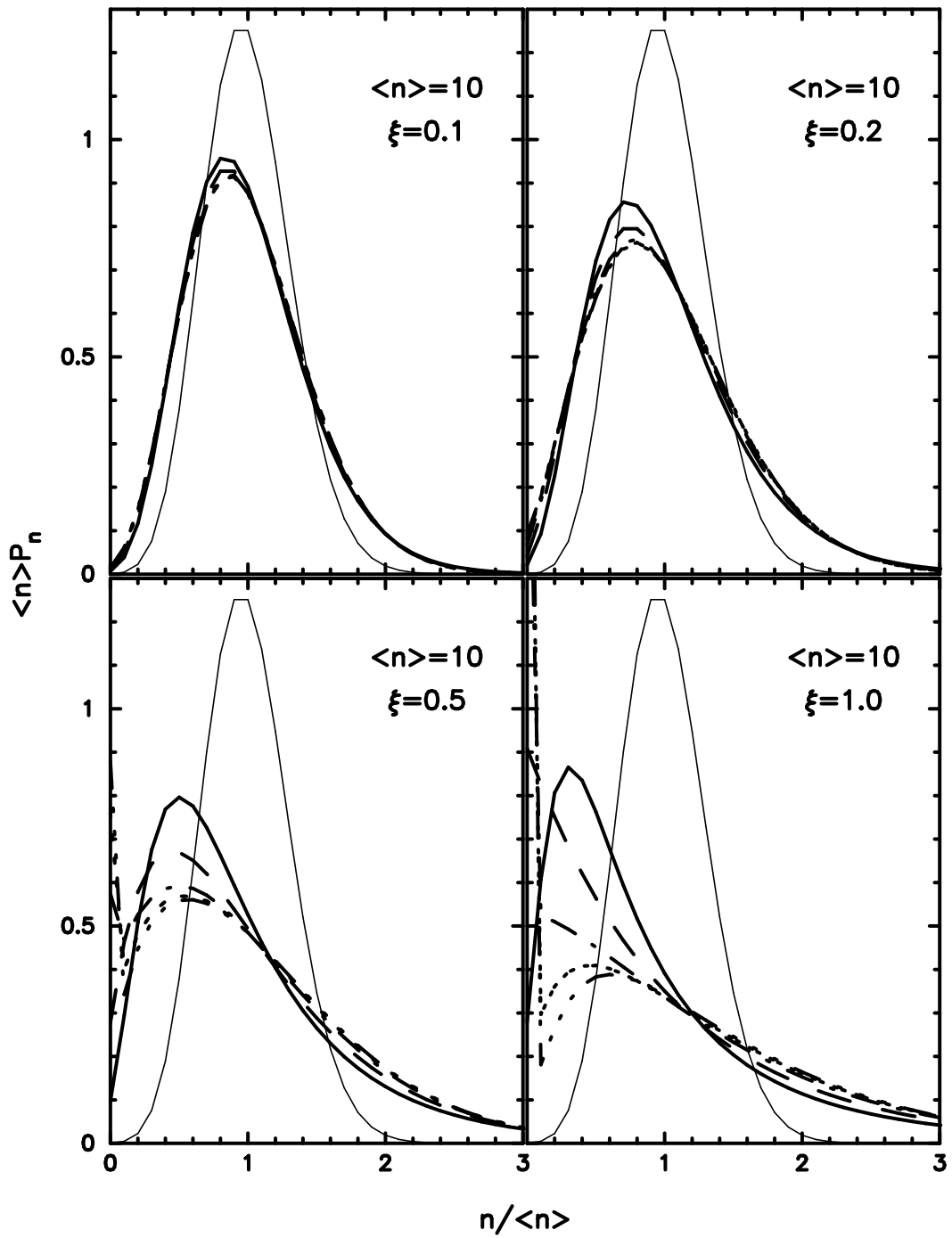


FIG. 5. P_n for fixed $\langle n \rangle = 10$ and for $a = 1/2, 1, 2, 3, 4$. The value $\xi = f_2/\langle n \rangle^2$ are shown in each figure. The various choices of a for each curve are given in the figure caption of Figs. 3 and 4.

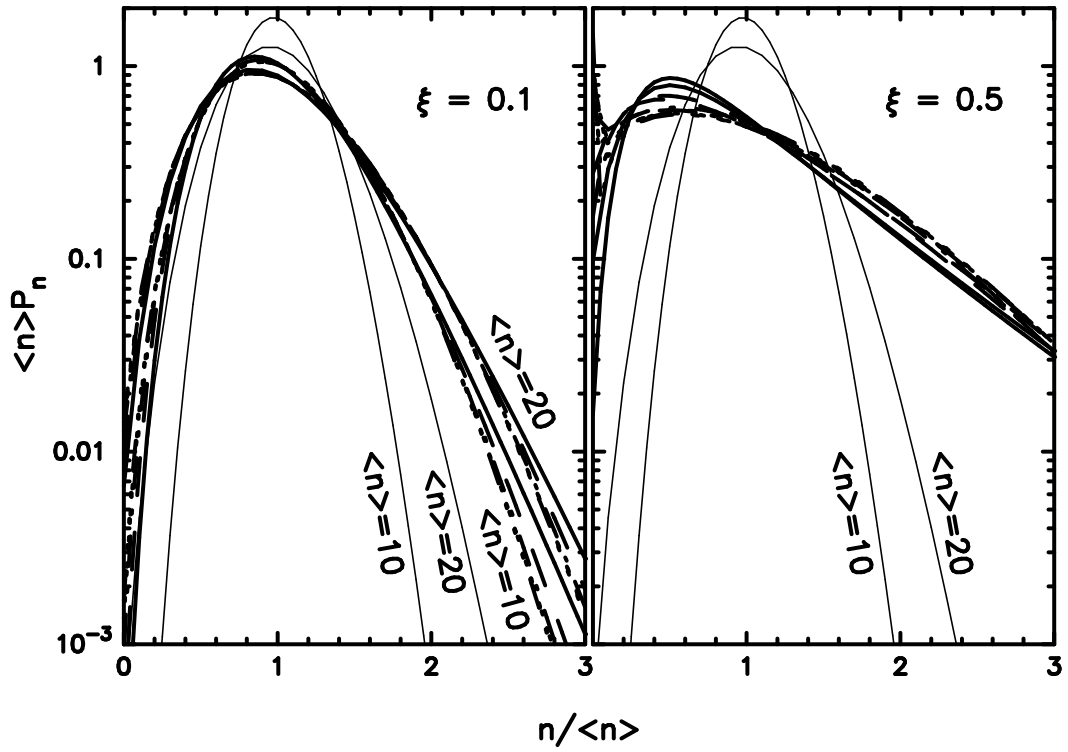


FIG. 6. KNO plot of $\langle n \rangle P_n$ for fixed $\langle n \rangle = 10$ and 20 for $a = 1/2, 1, 2, 3, 4$.

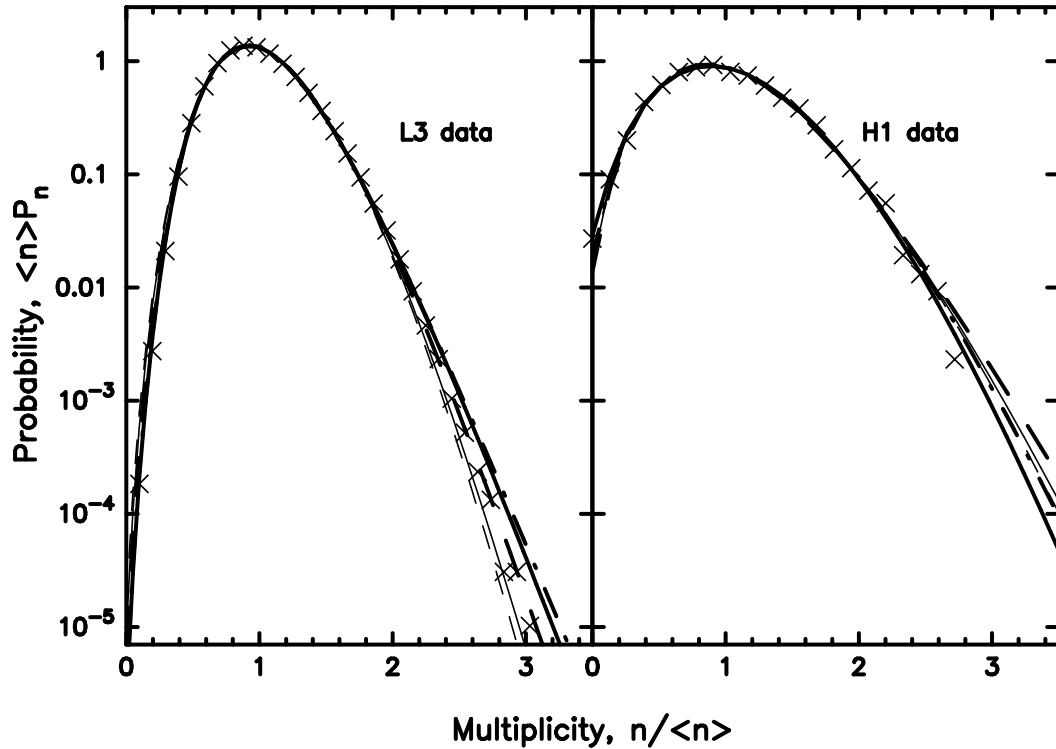


FIG. 7. Charged particle multiplicity distribution in jets of L3 data [40] and H1 data [41]. The crosses are the data and the curves are the fits with HGa and GRW1D given in Table III. The thick solid curves are the GRW1D fit, the thick dashed curves are LC model, the thin solid curves for NB model, the thin dashed curves for Geo model. The dash-dotted curves are for HGa model with $a = 0.31559$ for L3 data and with $a = 3.0$ for H1 data.

The KNO behavior for $\bar{n} \rightarrow \infty$ can also be studied for the models listed in Table I. According to KNO scaling, for distributions with a large mean value, the distribution $\langle n \rangle P_n$ becomes model independent in the new variable n/\bar{n} , i.e., variable scaled by mean value. In general, any distribution becomes Gaussian for large mean $\langle n \rangle$ according to the central limit theorem; specifically

$$P_n(\bar{n}, \sigma) = \frac{1}{\sqrt{2\pi\sigma^2}} \exp\left[-\frac{(n-\bar{n})^2}{2\sigma^2}\right] \\ = \left(1 + \frac{1}{\xi\bar{n}}\right)^{-1/2} \frac{1}{\bar{n}\sqrt{2\pi\xi}} \exp\left[-\frac{1}{2\xi}\left(\frac{n}{\bar{n}} - 1\right)^2 \left(1 + \frac{1}{\xi\bar{n}}\right)^{-1}\right] \quad (91)$$

with the mean $\langle n \rangle = \bar{n}$ and the standard deviation σ which is related to the reduced factorial cumulant ξ by $\sigma^2 = \langle n^2 \rangle - \langle n \rangle^2 = \bar{n} + \xi\bar{n}^2$. This means that the KNO scaling follows when the fluctuation is given by $\sigma^2 = \xi\bar{n}^2$ with a constant ξ or when $\xi\bar{n} \gg 1$. Thus to compare KNO scaling properties of $\bar{n}P_n$ for different models, the fluctuation of these models should have the same value of $\xi = f_2/\bar{n}^2$. For a small ξ , the Poisson component of the fluctuation $\sigma^2 = \bar{n} + \xi\bar{n}^2$ becomes dominant and thus the KNO scaling behavior is broken. For large ξ the Poisson component is negligible and KNO scaling is realized, i.e.,

$$\bar{n}P_n(\bar{n}, \xi) = \frac{1}{\sqrt{2\pi\xi}} \exp\left[-\frac{1}{2\xi}\left(\frac{n}{\bar{n}} - 1\right)^2\right] \quad (92)$$

The KNO plot of Fig.6 shows that the various distributions have no KNO scaling property for small fluctuation ($\xi = 0.1$) but show a KNO scaling property for large fluctuation ($\xi = 0.5$). The effect of mean on $\bar{n}P_n$ is larger than the difference between different model for $\xi = 0.1$ while the effect of mean on $\bar{n}P_n$ is much smaller than the difference between different models exhibiting KNO scaling behavior for $\xi = 0.5$. Ref. [33] shows the total charge distribution in hadronic collisions studied using SN model. From their fits we can extract the corresponding fluctuation which are $\xi = 0.05 \sim 0.5$ and $\bar{n} = 6 \sim 13$. This means that the KNO scaling behavior is marginal for these data, i.e., just fitting the distribution $\bar{n}P_n$ of the data does not show clear evidence for KNO scaling. We need to evaluate the explicit values of the mean number \bar{n} and the fluctuation ξ to check the KNO behavior of this data; the value of $\xi\bar{n}$ should be large enough to show KNO scaling behavior as can be seen from Eqs.(91) and (92). Table III shows that $\xi < 0.1$ and $\xi\langle n \rangle < 1$ for both data indicating that the KNO scaling behavior would not be clearly exhibited in jets for L3 and H1.

C. Sequential procedures and compound Poisson distributions

A Poisson distribution plays a very important role in physics. As already noted, in statistical physics, Maxwell-Boltzmann statistics leads to Poisson probabilities. Other distributions are compared to the Poisson distribution which acts as a benchmark for comparison. The distributions considered in this paper can have large non-Poissonian fluctuations. The purpose of this section is to show how they can be rewritten as a compound process or sequential process involving one aspect that has a Poisson character. As an example the negative binomial distribution can be obtained from a compound Poisson-logarithmic distribution as discussed in Ref. [33]. Here, we extended this result to include the other distributions and we also show that the final distribution can be obtained from compounding it with another distribution, such as the negative binomial. In general, the underlying picture for a sequential process involves a two step procedure in which the observed particles arise from the production of “clusters” with the subsequent decay of each cluster producing its distribution of particles. The final distribution is obtained by compounding the probability distribution of the clusters with another distribution coming from each cluster and summing over clusters. Specifically, the observed particles or members in system arise from production of $M = c$ clusters with probability distribution P_c . This is sequentially followed by each cluster decaying into k_α particles with the probability P_{k_α} with $\alpha = 1, 2, \dots, c$. The probability of observing $n = \sum_k k n_k = \sum_\alpha k_\alpha$ particles is then obtained by a compound probability expression

$$P_n = \sum_c \sum_{\{k_\alpha\}} P_c \prod_{\alpha=1}^c P_{k_\alpha} \quad (93)$$

A negative binomial distribution can be obtained when $P_c = \langle c \rangle^c e^{-\langle c \rangle} / c!$ and $P_{k_\alpha} = (q^{k_\alpha} / k_\alpha) / \ln(1/p)$. Here $c = M = \sum_k n_k$ and $\langle c \rangle = \langle M \rangle$, $p = (1 - z) = (1 + \langle n \rangle / x)^{-1}$ and $q = 1 - p = z = (\langle n \rangle / x) / (1 + \langle n \rangle / x)$. Also $N_c = \langle c \rangle = x \ln(1 + \langle n \rangle / x)$ and $n_c = \langle n \rangle / N_c = (\langle n \rangle / x) / \ln(1 + \langle n \rangle / x)$. This structure can be generalized as follow.

Since the generator of Poisson distribution is an exponential, i.e., the expansion of exponential gives the Poisson's distribution $P_n^P(\bar{n})$,

$$e^{\mathcal{N}} = \sum_{M=0}^{\infty} \frac{\mathcal{N}^M}{M!} = e^{\mathcal{N}} \sum_M e^{-\mathcal{N}} \frac{\mathcal{N}^M}{M!} = e^{\mathcal{N}} \sum_{M=0}^{\infty} P_M^P(\mathcal{N}) \quad (94)$$

The grand partition function or the generating function $Z = e^{f_0}$ for any distribution can be represented as a Poisson distribution whose mean value is the void variable f_0 or the grand potential $\Omega = -f_0$. On the other hand and in general we can rewrite the void variable as

$$f_0(\vec{x}) = \ln Z(\vec{x}) = \sum_k x_k = \mathcal{N} \sum_k \mathcal{P}_k(\vec{x}) \quad (95)$$

where $\mathcal{N} = f_0 = \sum_k x_k$ and

$$\mathcal{P}_k(\vec{x}) = \frac{x_k}{\mathcal{N}} \quad (96)$$

The $\mathcal{P}_k(\vec{x})$ can be connected to its generating function $\mathcal{G}(\vec{x}, u)$:

$$\mathcal{G}(\vec{x}, u) = \sum_k (1-u)^k \mathcal{P}_k(\vec{x}) = \frac{1}{\mathcal{N}} \sum_k x_k (1-u)^k \quad (97)$$

Thus the generating function $G(\vec{x}, u)$ of P_n can be expanded in terms of \mathcal{P}_k as

$$\begin{aligned} G(\vec{x}, u) &= \sum_n (1-u)^n P_n(\vec{x}) = \frac{1}{Z(\vec{x})} \sum_n Z_n(\vec{x}) (1-u)^n = \frac{e^{\mathcal{N}\mathcal{G}(\vec{x}, u)}}{e^{\mathcal{N}}} \\ &= \sum_{M=0}^{\infty} \frac{1}{e^{\mathcal{N}}} \frac{[\mathcal{N}\mathcal{G}]^M}{M!} = \sum_M P_M^P(\mathcal{N}) \left[\sum_j (1-u)^j \mathcal{P}_j \right]^M \\ &= \sum_M P_M^P(\mathcal{N}) \sum_{\vec{n}_M} \prod_k [(1-u)^k \mathcal{P}_k]^{n_k} \end{aligned} \quad (98)$$

where $P_M^P(\mathcal{N}) = e^{-\mathcal{N}} \mathcal{N}^M / M!$ is the Poisson distribution with the mean of $\mathcal{N} = f_0$. Here the sum over \vec{n}_M is the sum over partitions \vec{n} with a fixed $M = \sum_k n_k$. Thus we have

$$P_n(\vec{x}) = \sum_M P_M^P(\mathcal{N}) \sum_{\vec{n}_M} \prod_k \mathcal{P}_k^{n_k}(\vec{x}) \quad (99)$$

with $M = \sum_k n_k$ and $n = \sum_k k n_k$. Any distribution obtained from a generating function of the form of $Z(\vec{x}) = e^{f_0} = \exp[\sum_k x_k]$ can therefore be decomposed as a compound Poisson's distribution with some other distribution $\mathcal{P}_k = x_k / f_0$ obtained from the weight x_k .

The sequential nature of a process is explicitly shown on Eq.(99). The observed particle multiplicity distribution arises from a two step process in which $M = \sum_k n_k$ clusters are first distributed according to a Poisson distribution. This is then sequentially followed by breaking each of the n_k clusters of type k into k particles with probability $\mathcal{P}_k = x_k / \mathcal{N}$ and with $n = \sum_k k n_k$. The probability associated with a given M and \vec{n} with \vec{x} is $P_M(\vec{x}, \vec{n}) = P_M^P(\mathcal{N}) \prod_k \mathcal{P}_k^{n_k} = P_M^P(\mathcal{N}) \prod_k (x_k / \mathcal{N})^{n_k}$.

As an illustration we consider the LC model with $x_k = x C_k z^k / 2^{2(k-1)}$. Using the evolutionary variables [31] $x = \beta / 4p$ and $z = 4p(1-p)$ then $\mathcal{N} = \sum x_k = \beta$ for $p \leq 1/2$ as already noted in Sect. II E so that $P_M^P = e^{-\beta} \beta^M / M!$. The $x_k = \beta C_k p^{k-1} (1-p)^k$ so that $\mathcal{P}_k = x_k / \mathcal{N} = C_k p^{k-1} (1-p)^k$. The underlying diagram associated with \mathcal{P}_k are shown in Fig.2. For a negative binomial (NB) distribution, $x_k = x z^k / k$ and thus $\mathcal{P}_k = x_k / \mathcal{N}$ is generated from $\mathcal{N} = \sum_k x_k = -x \ln(1-z)$. Therefore the NB is a compound Poisson-Logarithmic distribution as shown in Table IV.

As another example, we consider the HGa model with general a instead of $a = 1/2$ for LC or $a = 1$ for NB. The weight x_k has the structure of the probability $P_k(x, z)$ of NB distribution given by Eq.(90), i.e.,

$$x_k = x \frac{z^k \Gamma(a+k-1)}{k! \Gamma(a)} = \frac{x}{a-1} \frac{1}{(1-z)^{a-1}} P_k^{\text{NB}}(a-1, z) \quad (100)$$

thus $\mathcal{P}_k = [1 - (1 - z)^{a-1}]^{-1} P_k^{\text{NB}}$ for HGa. Therefore the HGa \mathcal{P}_n distribution is a compound Poisson-NB distribution. This may be interpreted as a sequential process in which clusters with a Poisson cluster distribution P_c breakup into particles with a particle distribution \mathcal{P}_k given by a NB distribution with parameter a . For the various models considered here with their x_k listed in Table I, the corresponding distribution \mathcal{P}_k and the normalization factor $\mathcal{N} = f_0$ are listed in Table IV. We can further see that HGa can be looked as a compound Poisson-Poisson-Logarithmic distribution, i.e., a distribution having three sequential steps; Poissonian breakup into clusters \rightarrow Poissonian breakup of each cluster \rightarrow logarithmic breakup of each of them.

TABLE IV. Poissonian sequential distribution for various models of Table I.

Model	Weight \mathcal{N}	Distribution \mathcal{P}_k	Comments on \mathcal{P}_k
P	$\langle n \rangle$	$\frac{1}{\langle n \rangle}$	Monomer only or Uniform for N species
Geo	$x \frac{z}{1-z}$	$(1-z)z^{k-1}$	Uniform with constituents
NB	$x \ln \left(\frac{1}{1-z} \right)$	$\frac{z^k}{k} / \ln \left(\frac{1}{1-z} \right)$	logarithmic with constituents
LC	$2x [1 - \sqrt{1-z}]$	$\left[\frac{1/2}{1-\sqrt{1-z}} \right] \frac{z^k}{k!} \frac{\Gamma(k-1/2)}{\Gamma(1/2)}$	NB with constituents with $\mathcal{P}_0 = 0$
HGa	$\frac{x}{1-a} [1 - (1-z)^{1-a}]$	$\left[\frac{(1-z)^{1-a}}{(1-z)^{1-a}-1} \right] P_k^{\text{NB}}(a-1, z)$	NB with constituents without $k = 0$
GRW1D	$\frac{xz}{(1-z)^a}$	$P_{k-1}^{\text{NB}}(a, z)$	NB with $x = a$
$x_k = \frac{x}{k!} z^k$	$x e^{az}$	$e^{-az} \frac{z^k}{k!}$	Poisson (exponential)

Because of a unique role played by the Poisson distribution and the form $e^{f_0} = \exp[\sum_k x_k]$ of the generating function, the cluster distribution P_c is usually taken to be a Poisson. However, as noted before, other divisions are possible. Using the same approach used above for $P_c = P_M^P$, we can expand any distribution using a NB instead of Poisson, i.e., with $P_c = P_M^{\text{NB}}$ using the form of the generating function $Z(x, z) = (1 - z)^{-x}$ for the NB. Replacing z by $\mathcal{N}(z)$, the normalization factor of a new distribution, we have

$$Z(x, z) = [1 - \mathcal{N}(z)]^{-x} = [1 - \mathcal{N}(z)\mathcal{G}(u = 0)]^{-x} \quad (101)$$

The $\mathcal{G}(u)$ is

$$\mathcal{G}(u) = \frac{\mathcal{N}([1 - u]z)}{\mathcal{N}(z)} = \sum_k (1 - u)^k \mathcal{P}_k \quad (102)$$

while the $G(u)$ is

$$G(u) = \sum_n (1 - u)^n P_n = \frac{Z(x, [1 - u]z)}{Z(x, z)} = \frac{[1 - \mathcal{N}\mathcal{G}(u)]^{-x}}{[1 - \mathcal{N}]^{-x}} \quad (103)$$

Thus we have

$$\begin{aligned} G(u) &= \sum_{M=0}^{\infty} (1 - \mathcal{N})^x \frac{\mathcal{N}^M \Gamma(x + M)}{M! \Gamma(x)} [\mathcal{G}(u)]^M = \sum_{M=0}^{\infty} P_M^{\text{NB}}(x, \mathcal{N}) [\mathcal{G}(u)]^M \\ &= \sum_{M=0}^{\infty} P_M^{\text{NB}} \left[\sum_{j=0}^{\infty} (1 - u)^j \mathcal{P}_j \right]^M = \sum_{M=0}^{\infty} P_M^{\text{NB}} \sum_{\{n_k\}_M} \prod_k [(1 - u)^k \mathcal{P}_k]^{n_k} \end{aligned} \quad (104)$$

$$P_n(\vec{x}) = \sum_M P_M^{\text{NB}}(x, \mathcal{N}) \sum_{\{n_k\}_M} \prod_k \mathcal{P}_k^{n_k}(\vec{x}) \quad (105)$$

The result of Eq.(105) shows that the distribution P_n can be written as a compound probability distribution of a negative binomial P_M^{NB} with another probability \mathcal{P}_k distribution generated from $\mathcal{G}(u)$. For the case of $\mathcal{N}(z) = e^z$, which may be considered as the fugacity $e^z = e^\mu$ for a particle with chemical potential $\mu = z$, \mathcal{G} can further be decomposed as

$$\mathcal{G}(u) = \frac{\mathcal{N}((1 - u)z)}{\mathcal{N}(z)} = \frac{e^{(1-u)z}}{e^z} = \sum_{k=0}^{\infty} (1 - u)^k P_k^P(z) \quad (106)$$

i.e., \mathcal{P}_k for this case is Poisson $P_k^P(z)$. If $\mathcal{N} = 1 - e^{f_0/x}$, then $\mathcal{P}_k = P_k^P(f_0/x)$ without $k = 0$ and $Z(x, z) = [1 - (1 - e^{f_0/x})]^x = e^{f_0}$. For $f_0 = \sum_k x_k$ given in Table I, the \mathcal{P}_k becomes the same probability with x_k replaced by x_k/x . As an example the HGa with $Z(x, z) = \exp\left(\frac{x}{1-a}[1 - (1 - z)^{1-a}]\right)$ can be decomposed as a sequential process consisting of a NB distribution of clusters with $Z(x, \mathcal{N} = 1 - e^{f_0/x})$ which is then followed by a breakup of clusters distributed with a HGa distribution with $Z(x = 1, z)$ but without voids, i.e., with $\mathcal{P}_0 = 0$. Thus this decomposition separates the parameter x assigned to cluster from other parameters.

IV. CONCLUSION

Event-by-event studies from high energy collisions are being used to study the details of particle multiplicity distributions as, for example, those associated with pions. Such studies not only give information about the mean number of particles produced, but also information about fluctuations and higher order moments of the probability distribution which are important tools for studying the underlying processes and mechanisms that operate. They are also useful in distinguishing various phenomenological models. Issues associated with fluctuations play an important role in many areas of physics and departures from Poisson statistics are of current interest. One purpose of this paper was an investigation of various models of particle multiplicity distributions that can be used in event-by-event analysis. These various phenomenological models are developed using a general form of a unified model which is based on a grand canonical partition function and an underlying weight arising from Feynman's path integral approach to

statistical processes. A resulting distribution has three control parameters called a , x , z . The relationships of these parameters to various physical quantities are discussed. One important result is the connection of the parameter a to the Fisher exponent τ ; namely $\tau = 2 - a$ for HGa. This connection arises from a parallel we developed between the model for particle multiplicity distributions considered here and our previous approach to cluster yields. Since an exact description of particle multiplicity distributions is not known, we have considered several cases with different τ 's or a 's which are contained in our unified description. Moreover, many of the existing distributions currently used in particle phenomenology are shown to be special choices of τ or a which appear in a generalized hypergeometric model called HGa. These include the Poisson distribution coming from coherent emission, chaotic emission producing a negative binomial distribution, combinations of coherent and chaotic processes leading to signal/noise distributions and field emission from Lorentzian line shapes producing the Lorentz/Catalan distribution. Using the HGa model combinants, cumulants and moments are discussed and a physical significance is given to combinants in terms of the underlying partition weights of a Feynman path integral approach to statistical processes. The parameter a or Fisher exponent τ is shown to play an important role in the behavior of the combinants which manifest itself in various physical relationships. The HGa model and its associated special cases are used to explore a wide variety of phenomena. These include: linked pair approximations leading to hierarchical scaling relations on the reduced cumulant level, generalized void scaling relations, clan variable descriptions and their connections with stochastic variables and branching processes, KNO scaling behavior, enhanced non-Poissonian fluctuations. Models based on an underlying random walk description are also discussed.

In this paper we compared various particle multiplicity distributions within the hypergeometric model HGa. Our results show that even though various distributions have the same mean and fluctuation, the distribution itself or the underlying mechanism could be different. Comparisons within the HGa model also show that just comparing void variables χ and ξ or mean \bar{n} and fluctuation f_2 or σ is not enough to distinguish different models that describe particle multiplicity data. Thus, to find the correct distribution and underlying mechanism from various data more information than just the mean and fluctuation are necessary and new variables should be found which are quite different between different models. For example, higher order reduced factorial cumulants need also to be evaluated such as the third order cumulant κ_3 .

Applications of our approach to the charged multiplicity data of L3 and H1 are given. The mean $\langle n \rangle$, fluctuation variable ξ , void scaling variable χ , and third order reduced cumulant variable κ_3 obtained from these experiments are compared with various models discussed in this paper. The value of the third cumulant κ_3 shows that the GRW1D model can fit the charge multiplicity data of L3 and H1. The HGa model also gives a fit to the L3 data, but is not as successful as GRW1D with respect to the third order reduced cumulant of the H1 data. Both have very similar multiplicity distributions as shown in Fig.7 which compares the two models with the charged particle multiplicity distributions of jets for L3 and H1 data. Differences appear in the high multiplicity events with reduced multiplicity $n/\langle n \rangle > 2.5$. The reduced third cumulant is negative for the H1 data of Table III. Negative values of a cumulant require negative values of the parameter a which are allowed in GRW1D if the parameters x and z are also taken as negative, but a negative value of a is not acceptable in HGa since this would require a value of z greater than 1 and thus a complex x . We also discuss the KNO scaling behavior for these data and conclude that the KNO scaling behavior would not be clearly exhibited in the jets for L3 and H1.

In this paper we have also generalized the compound distribution that arises from sequential process which may reveal the dynamical structure of the distribution. Specifically, the underlying sequential picture involves a two step process where the final distribution arises from the production of clusters followed by a subsequent decay of the clusters. For the HGa model, the final distribution is obtained from compounding a Poisson distribution of clusters with a NB distribution coming from the decay of each of the clusters. The HGa may arise through a three step sequential process of Poisson-Poisson-Logarithmic compound distribution. It is also shown that the HGa can arise from a two step sequential process of a NB distribution followed by a new HGa with a different mean value.

This work was supported in part by Grant No. 2001-1-11100-005-3 from the Basic Research Program of the Korea Science and Engineering Foundation and in part by the DOE Grant No. DE-FG02-96ER-40987.

-
- [1] K. Rajagopal and F. Wilczek, Nucl. Phys. **B404**, 557 (1993).
 - [2] S. Gavin and B. Müller, Phys. Lett. **B329**, 486 (1994).
 - [3] G. Bayer and H. Heiselberg, Phys. Lett. **B469**, 7 (1999).
 - [4] V. Heinz and B.V. Jacak, Ann. Rev. Nucl. Part. Sci., **49**, (1999).
 - [5] S. Pratt, Phys. Lett. **B301**, 159 (1993).

- [6] Csörgö and J. Zimanyi, Phys. Rev. Lett. **80**, 916 (1998).
- [7] H.R. Andrews, C.G. Townsend, H.J. Meisner, D.S. Durfee, D.M. Korn, W. Ketterle, Science **275**, 637 (1997).
- [8] A. Bialas and R. Peschanski, Nucl. Phys. **B272**, 703 (1986); **B306**, 857 (1988).
- [9] P. Carruthers and C.C. Shih, Phys. Lett. **127B**, 242 (1983).
- [10] L. Van Hove, Phys. Lett. **B232**, 509 (1989).
- [11] L. Van Hove and A. Giovannini, Z. Phys. **C30**, 391 (1988).
- [12] Z. Koba, H.B. Nielson and P. Olesen, Nucl. Phys. **B40**, 317 (1972).
- [13] P. Carruthers and I. Sarcevic, Phys. Lett. **B189**, 442 (1987).
- [14] M. Gaździcki and S. Mrówczyński, Z. Phys. **C54**, 127 (1992).
- [15] M. Stephanov, K. Rajagopal, E. Shuryak, Phys. Rev. Lett. **81**, 4816 (1998).
- [16] M.A. Hiasz, A.D. Jackson, R.E. Shrock, M.A. Stepanov, and J.J.M. Verbaarschot, Phys. Rev. **D58**, 96007 (1998).
- [17] G. Baym and H. Heiselberg, Phys. Lett. **B469**, 7 (1999).
- [18] S. Jeon and V. Koch, Phys. Rev. Lett. **83**, 5435 (1999); Phys. Rev. Lett. **85**, 2076 (2000).
- [19] M. Asakawa, U. Heinz and B. Müller, Phys. Rev. Lett. **85**, 2072 (2000).
- [20] H. Heiselberg and A.D. Jackson, Phys. Rev. **C63**, 064904 (2001).
- [21] A.Z. Mekjian and S.J. Lee, Phys. Rev. **A44**, 6294 (1991).
- [22] S.J. Lee and A.Z. Mekjian, Phys. Rev. **C45**, 1284 (1992).
- [23] S.J. Lee and A.Z. Mekjian, Phys. Rev. **C45**, 365 (1992).
- [24] S.J. Lee and A.Z. Mekjian, Phys. Rev. **C56**, 2621 (1997).
- [25] S.J. Lee and A.Z. Mekjian, Phys. Rev. **C47**, 2266 (1993).
- [26] S.J. Lee and A.Z. Mekjian, Phys. Rev. **C50**, 3025 (1994).
- [27] K.C. Chase and A.Z. Mekjian, Phys. Rev. **C 49**, 2164 (1994); **50**, 2078 (1994).
- [28] S. Lupia, A. Giovannini, and R. Ugoccioni, Z. Phys. **C59**, 427 (1993).
- [29] M. Gyulassy and S. Kaufmann, Phys. Rev. Lett. **40**, 298 (1978); J. Phys. **A11**, 1715 (1978).
- [30] A.Z. Mekjian, B.R. Schlei and D. Strottman, Phys. Rev. **C58**, 3627 (1998).
- [31] A.Z. Mekjian, Phys. Rev. Lett. **86**, 220 (2001).
- [32] A. Mekjian, Phys. Rev. **C65**, 014907 (2002).
- [33] P. Carruthers and C.C. Shih, Int. J. Modern Phys. **A2**, 1447 (1987).
- [34] F. Becattini, A. Giovannini and S. Lupia, Z. Phys. **C72**, 43 (1996).
- [35] R. Hwa, in *Proc. of the Santa Fe Workshop on Intermittency in High Energy Collisions* (World Scientific, Singapore, 1990, F. Cooper, R. Hwa and I. Sarcevic, Edit).
- [36] S. Hegyi, Phys. Lett. **B309**, 443 (1993); **B318**, 642 (1993).
- [37] R.P. Feynman, *Statistical Physics* (Benjamin/Cummings, New York, 1972).
- [38] J. Klauder and E.C.G. Sudarshan, *Fundamentals of Quantum Optics* (Benjamin, N.Y., 1968).
- [39] H. Biyajima, Prog. Theo. Physics **69**, 966 (1983).
- [40] L3 collaboration, LANL preprint hep-ex/0110072 (2001).
- [41] S. Aid et al., H1 collaboration, Z. Phys. **C72**, 573 (1996); LANL hep-ex/9608011 (1996).